Lateral Membrane-Specific MAGUK CASK Down-Regulates NaV 1.5 Channel in Cardiac MyocytesNovelty and Significance

Catherine A. Eichel, Adeline Beuriot, Morgan Y.E. Chevalier, Jean-Sébastien Rougier, Florent Louault, Gilles Dilanian, Julien Amour, Alain Coulombe, Hugues Abriel, Stéphane N. Hatem, et al.

The lateral membrane-specific MAGUK CASK down-regulates $Na_V1.5$ channel in cardiomyocytes

Eichel

Negative regulation of $Na_V1.5$ by the MAGUK CASK

Catherine A. Eichel, PhD[1], Adeline Beuriot, MSc[1], Morgan Y.E. Chevalier, MSc[3], Jean-Sébastien Rougier, PhD[3], Florent Louault, MSc[1], Gilles Dilanian, MSc[1], Julien Amour, MD, PhD[1,2], Alain Coulombe, PhD[1], Hugues Abriel, MD, PhD[3], Stéphane N. Hatem, MD, PhD[1,2] and Elise Balse, PhD[1*]

[1]Sorbonne Universités - UPMC Univ Paris 06 - Inserm - UMR_S 1166 - Unité de recherche sur les maladies cardiovasculaires, le métabolisme et la nutrition - Faculté de Médecine - Site Pitié-Salpêtrière, 91 boulevard de l'Hôpital, 75013 PARIS - FRANCE
[2]Département de Cardiologie, Assistance Publique-Hôpitaux de Paris, Hôpital Pitié-Salpêtrière, PARIS - FRANCE
[3]Department of Clinical Research, University of Bern, Murtenstrasse 35, 3008 BERN - SWITZERLAND.

*Corresponding author:
Dr. Elise Balse, PhD
INSERM UMRS1166
Faculté de Médecine Pitié-Salpêtrière
91, Boulevard de l'Hôpital
75013 Paris
(tel) +33140779650
(fax) +33140779545
E-mail: elise.balse@upmc.fr

Total word count: 6789

- Basic Science Research
- Ion Channels/Membrane Transport
- Myocardial Biology
- Physiology

ABSTRACT:

Rationale: Mechanisms underlying membrane protein localization are crucial in the proper function of cardiomyocytes. The main cardiac sodium channel, $Na_V1.5$, carries the sodium current (I_{Na}) which provides a rapid depolarizing current during the upstroke of the action potential. While enriched in the intercalated disc (ID), $Na_V1.5$ is present in different membrane domains in myocytes and interacts with several partners.
Objective: To test the hypothesis that the Membrane-Associated GUanylate Kinase (MAGUK) protein CAlcium/calmodulin-dependent Serine protein Kinase (CASK) interacts with and regulates $Na_V1.5$ in cardiomyocytes.
Methods and results: Immunostaining experiments showed that CASK localizes at lateral membranes (LM) of cardiomyocytes, in association with dystrophin. Whole-cell patch clamp showed that CASK-silencing increases I_{Na} *in vitro*. *In vivo* CASK knockdown similarly increased I_{Na} recorded in freshly isolated myocytes. Pull-down experiments revealed that CASK directly interacts with the C-terminus of $Na_V1.5$. CASK silencing reduces syntrophin expression without affecting $Na_V1.5$ and dystrophin expression levels. Total Internal Reflection Fluorescence microscopy (TIRFm) and biotinylation assays showed that CASK silencing increased the surface expression of $Na_V1.5$ without changing mRNA levels. Quantification of $Na_V1.5$ expression at the LM and ID revealed that the LM pool only was increased upon CASK silencing. The protein transport inhibitor brefeldin-A prevented I_{Na} increase in CASK-silenced myocytes. During atrial dilation/remodeling, CASK expression was reduced but its localization unchanged.
Conclusion: This study constitutes the first description of an unconventional MAGUK protein, CASK, which directly interacts with $Na_V1.5$ channel and controls its surface expression at the LM by regulating ion channel trafficking.

Keywords: MAGUK, CASK, syntrophin, sodium channel, cardiomyocyte

Non-standard Abbreviations and Acronyms:

- MAGUK: Membrane Associated GUanylate Kinase
- CASK: Calcium/CAlmodulin-dependent Serine Kinase
- 3-D: 3-dimensionnal
- TIRFm: Total Internal Reflection Fluorescence microscopy
- shRNA: short hairpin RNA
- Ad: adenovirus
- D*IV*: Day *in vitro*
- BFA: brefeldin-A

INTRODUCTION

Cardiomyocytes are highly differentiated striated muscle cells possessing well-organized membrane domains with specialized roles in their electrical and mechanical functions. The T-tubule system and intercalated discs (ID) are the best characterized membrane domains and are crucial for the excitation-contraction (EC) coupling process and the propagation of action potentials (AP) from one myocyte to the other. Specialized membrane domains contain distinct populations of ion channels, pumps, exchangers and receptors such as the voltage-gated L-type calcium channel and gap-junction protein connexin-43, for T-tubules and ID respectively[1].

The main cardiac $Na_V1.5$ sodium channel is responsible for the sodium current I_{Na}, which provides a rapid depolarizing current during the upstroke of the AP. Recent studies suggest the presence of distinct populations of $Na_V1.5$ channel located in different specialized membrane domains of cardiomyocytes, as well as their association with specific partners. At the ID, $Na_V1.5$ has been shown to be associated with gap junctional (connexin-43)[2], desmosomal (plakophilin-2)[3,4], actin cytoskeleton-binding (ankyrin-G)[5,6], and Membrane-Associated GUanylate Kinase (MAGUK, SAP-97) proteins[7,8].

The mechanisms regulating the spatial organization of ion channels are still poorly understood. Targeting and clustering of transmembrane proteins to cell junctions are critical for the organization of specialized membrane domains in structurally polarized cells such as neurons, epithelial cells or cardiomyocytes. MAGUK proteins have emerged as key partners participating in this organization[9]. For instance, in the central nervous system, MAGUK proteins organize synapses through their ability to establish specific macromolecular complexes. In cardiomyocytes, SAP-97 is a key regulator of ion channel function and organization[7,8,10–13] whereas ZO-1 organizes the gap-junction protein connexin-43 at the ID[14]. Similar to other MAGUK proteins, CASK (Calcium/CAlmodulin-dependent Serine Kinase) displays a multidomain structure enabling interaction with multiple proteins including ion channels and receptors, cell-adhesion proteins and the actin cytoskeleton[9]. However, among MAGUK proteins, CASK differs due to the possession of an active CaMKII homolog domain in the N-terminal and a GUK (guanylate-kinase) domain in its C-terminus which is involved in CASK translocation to the nucleus and subsequent regulation of gene expression[15]. Despite previous works reporting the expression of CASK in the myocardium[16,17], its function has not been investigated. Therefore, we investigated the potential role of CASK in the regulation of $Na_V1.5$ channels in cardiomyocytes.

Here we present the first detailed characterization of the localization and function of CASK in the heart. CASK was detected specifically in costameric structures of the lateral membrane (LM) of cardiomyocytes, in association with dystrophin. Using a combination of whole-cell patch-clamp, high resolution 3-dimensional deconvolution microscopy and biochemistry, we showed that CASK interacts with $Na_V1.5$ and negatively regulates the corresponding current in cultured adult atrial myocytes. CASK knock down *in vivo* revealed that CASK exerted the same regulatory function in freshly isolated ventricular myocytes. Pull down assays showed that CASK directly interacts with the C-terminus of $Na_V1.5$. Biotinylation and Total Internal Reflection Fluorescence (TIRF) microscopy revealed that CASK silencing increased $Na_V1.5$ expression at the cell surface without changing $Na_V1.5$ mRNA and protein levels. However, CASK silencing reduced the expression of syntrophin. The I_{Na} increase induced by CASK silencing was completely prevented by the protein transport inhibitor brefeldin-A, suggesting the involvement of CASK in trafficking processes. Finally, we showed that CASK expression is reduced in remodeled/dilated atrial biopsies without changes in localization. These results not only strengthen the concept of differentially regulated pools of $Na_V1.5$ channels within the cardiomyocyte playing distinct roles in cardiac physiology, but also suggest that CASK could participate in maintaining low levels of $Na_V1.5$ at the LM and consequently contribute to anisotropic conduction.

METHODS

An expended Methods section is available in the Online Data Supplement.

Cell preparations, Transfections and Adenoviral infections

Adult atrial or ventricular myocytes were obtained by enzymatic dissociation on a Langendorff column as previously described[18]. Adult rat atrial myocytes were infected with Ad-shscr, Ad-shCASK, Ad-GFP or Ad-CASK. HEK293 cells stably expressing $Na_V1.5$ were transiently transfected with either shscr or shCASK and pIRES-GFP or pIRES-GFP-CASK.

Cardiac-specifc CASK knockdown mouse

Mice were generated by Cre/loxP-mediated gene targeting through homologous recombination. The homozygous floxed $CASK^{tm1Sud}$ mouse was bred with a cardiomyocyte-specific Cre-recombinase mouse, α myosin heavy chain (αMHC)-Cre.

Semi-quantitative real-time PCR

Details of specific primers designed to amplify *cask*, *scn5a* and housekeeping genes are described in the Online Data Supplement.

Protein extraction, Western Blot and Pull-down assays

These procedures were performed as previously reported[8,18]. See Online Data Supplement for other details.

Deconvolution microscopy, Evanescent field microscopy and Image analysis

3-D deconvolution epifluorescence and TIRF microscopy images were acquired as described previously[18]. Analysis was performed using ImageJ software (NIH). Details are given in the Online Data Supplement.

Electrophysiological measurements

Patch-clamp recordings were performed in the whole-cell configuration at room temperature. Detailed solutions and protocols are available in the Online Data Supplement.

Human samples

In accordance with approval of Institution Ethic Committee, biopsies of right atrial appendages were obtained from patients undergoing cardiac surgery. See Online Data Supplement.

Statistics

Data are represented as mean±SEM; *: $P<0.05$, **: $P<0.01$ and ***: $P<0.001$; ^{ns}: not significant.

RESULTS

The MAGUK CASK is expressed at the lateral membrane and excluded from the intercalated disc.

We first looked at the expression of CASK in adult myocardium by western blot. CASK was expressed both in rat atria and ventricle lysates, with a ~2 fold larger expression in atria. CASK was also expressed in myocyte- and fibroblast-enriched fractions (Figure 1A-B). Secondly, we examined the localization of CASK in rat atrial and ventricular myocardial cryosections using high resolution 3-dimensional (3-D) deconvolution microscopy. In ventricle, CASK was expressed along the LM stained with caveolin3 (Figure 1C, top panel) whereas no signal was detectable at the intercalated disc (ID) stained with N-cadherin (Figure 1C, middle). CASK also exhibited a striated pattern, facing the sarcomeric α-actinin corresponding to z-line (Figure 1C, bottom panel), suggesting either a T-tubular or a costameric localization. The distribution of

CASK regarding the different compartments of cardiomyocytes was similar in the atrial myocardium (Online Figure I).

CASK is a new member of the dystrophin-glycoprotein complex at the lateral membrane of cardiomyocytes.

In freshly isolated myocytes, CASK staining was apparent along the LM and exhibited the z-line superposition reported above. To investigate whether CASK was located at the T-tubule, co-immunofluorescence experiments were conducted with $Ca_V1.2$ or RyR2. However, little co-localization was observed in myocytes (Online Figure IIA). In addition, after detubulation by formamide treatment, the striated pattern was still observed in live ventricular myocytes stained with the voltage-sensitive dye Di-8-ANEPS (Online Figure IIB).

Next, the association of CASK with either vinculin or dystrophin costameric complexes was investigated in freshly isolated adult atrial myocytes (Figure 2A-B). CASK more closely associated with dystrophin (R: 0.68) than with vinculin (R: 0.31) (Figure 2A). In contrast with vinculin which is organized in rib-like structures at the sarcolemma, CASK showed a continuous layering of the sarcolemma, similar to dystrophin (Figure 2B). In addition, CASK and dystrophin displayed a regular interval alignment of ~2 µm, the interval between two z-lines, in the midsection of cardiomyocytes (Figure 2C). The association between CASK and dystrophin was further supported by co-immunoprecipitation experiments performed on whole heart lysates (Figure 2D). Finally, immunostainings performed on dystrophin-deficient mdx mouse ventricular cryosections showed a loss of CASK staining, suggesting that CASK expression at the LM of cardiomyocytes depends on dystrophin expression (Figure 2E). Note that the striated distribution of CASK was not observed in mouse myocardium, suggesting distinct costameric organization between species.

Altogether, these results indicate that CASK is poorly expressed at the T-tubule under normal conditions and is a new member of the dystrophin-glycoprotein complex.

CASK directly interacts with $Na_V1.5$.

Since $Na_V1.5$ associates with the dystrophin-glycoprotein complex at the LM[19], we explored the interaction of CASK with $Na_V1.5$. In freshly isolated atrial myocytes, CASK and $Na_V1.5$ exhibited both a sarcolemmal and striated expression and partially overlapped (R: 0.31) (Figure 3A-B). This partial overlap is likely due to high expression of $Na_V1.5$ channels at the ID where CASK is not present. Periodic intervals between two striations calculated using Fast Fourier Transform revealed a coherent distance of ~2 µm (Figure 3A). Of note, in this selected focal plane, the intercalated disc was not visible. The interaction between CASK and $Na_V1.5$ in the rat myocardium was supported by co-immunoprecipitation experiments (Figure 3C).

To investigate whether CASK could specifically interact with $Na_V1.5$, pull-down experiments were performed using the WT $Na_v1.5$ C terminus (Ct) or deleted for the PDZ binding motif corresponding to the 3 last SIV residues (ΔSIV, Figure 3D). Western blot experiments performed using anti-CASK and anti-pan syntrophin antibodies revealed that the $Na_V1.5$ WT Ct precipitated the two proteins from rat ventricle lysates. This interaction was dependent on the SIV motif of $Na_V1.5$ as interactions with CASK and syntrophin were respectively reduced by 94% and 61% with the truncated construct (Figure 3E). Finally, direct interaction between CASK and the $Na_V1.5$ Ct was investigated by performing pull-down experiments with the purified CASK protein (Figure 3F). At 10ng of purified CASK protein, the interaction was reduced by 21% but not abolished in ΔSIV.

These results support that CASK interacts directly with $Na_V1.5$ Ct, regardless of the presence of syntrophin, and that other residues than SIV are likely involved in this interaction.

CASK regulates the sodium current *in vitro*.

To assess the functional consequence of the interaction between CASK and $Na_V1.5$, I_{Na} was recorded in adult atrial myocytes using whole-cell patch-clamp after modulating the expression of CASK. Representative images of adenoviral infection efficiency in cultured rat atrial myocytes are presented Online Figure IIIA. CASK was overexpressed using an adenoviral

construct containing the GFP reporter (Ad-CASK) and compared to GFP alone (Ad-GFP). CASK mRNA was increased by 120% and protein level by 200% in Ad-CASK after 3 days *in vitro* (D*IV*) (Online Figure IIIB-D). Average current-voltage (I-V) plots from voltage clamp experiments showed a significant decrease in I_{Na} density at different tested voltages in Ad-CASK (Figure 4A-C). CASK overexpression shifted the steady-state inactivation curve leftward by ~8 mV ($P<0.001$, Figure 4E) whereas no difference was found for activation properties between Ad-CASK- and Ad-GFP-infected cells (Figure 4D). Next, we used adenoviral transfer technology to knockdown CASK in adult rat atrial myocytes. Silencing experiments were performed using GFP adenoviral construct containing a shRNA for CASK (Ad-shCASK) and compared to a scramble shRNA (Ad-shscr). CASK mRNA was decreased by 60% and protein level by 40% in Ad-shCASK at 5 D*IV* (Online Figure IIIB-D). Voltage clamp experiments showed a significant increase in I_{Na} at several tested voltages in Ad-shCASK (Figure 4B-F). No difference was found for activation properties between Ad-shCASK and Ad-shscr cells whereas steady-state inactivation was ~8 mV more positive in Ad-shCASK cells ($P<0.05$, Figures 4G-H). It is worth noting that the CASK-dependent shift in steady-state inactivation cannot explain the 2-fold change in I_{Na} density. These experiments clearly demonstrate that CASK exerted a repressive function on I_{Na}.

The regulatory function of CASK on I_{Na} is conserved *in vitro* from polarized cardiomyocytes to non-polarized HEK293 cells.

As CASK expression was restricted to the LM of cardiomyocytes, we investigated whether the regulatory function of I_{Na} by CASK could be dependent on the loss of structural polarity and dedifferentiation under culture conditions.

We followed the distribution of CASK in cardiomyocytes *in vitro* in accordance with the distribution of the adherens junction protein N-cadherin. Immediately after dissociation, CASK was absent from the ID where N-cadherin was confined. At D*IV*1, N-cadherin started to be internalized and at D*IV*2, was randomly distributed in the cytoplasm. At the same stage, CASK was located at the cell membrane. After one week in culture (D*IV*7), cardiomyocytes had reestablished contacts (ID-like structures) in which N-cadherin was located and CASK excluded (Online Figure IV). Therefore, CASK localization appeared related to the architecture/polarity of cardiomyocytes.

Thus, to investigate whether the regulation of I_{Na} by CASK could be polarity-dependent, we induced the formation of adherens junctions *in vitro*. Adult atrial myocytes infected with Ad-shscr or Ad-shCASK were seeded on Fc fragment plus N-cadherin (N-cadh) or Fc fragment alone, used as a control (Fc) (Online Figure VA). Atrial myocytes seeded on N-cadh showed both increased spreading and increased N-cadherin staining as shown by TIRF microscopy (Online Figure VA). Average I-V plots from voltage clamp experiments showed a significant increase in I_{Na} density at several tested voltages in the two coating conditions (Fc and N-cadh) in Ad-shCASK infected myocytes (Online Figure VB). No difference was found between Ad-shCASK myocytes cultured on N-cadh or Fc for activation properties whereas the steady-state inactivation curve was significantly shifted rightward in Ad-shCASK myocytes in the two coating conditions (~12 and 10 mV respectively, $P<0.05$) (Online Figure VC-D).

Next, I_{Na} was recorded in the non-polarized HEK293 cell line stably expressing cardiac $Na_V1.5$ α subunits (HEK293-$Na_V1.5$) (Online Figure VIA). We first overexpressed CASK using a GFP plasmid construct (CASK) and control HEK293-$Na_V1.5$ were transfected with GFP alone (GFP). CASK expression was 2-fold increased in CASK at 3D*IV* (Online Figure VIB-C). Average I-V plots from voltage clamp experiments showed a significant decrease in I_{Na} density in CASK compared with control cells (Online Figure VID). CASK overexpression shifted the steady-state inactivation curve by ~-6 mV ($P<0.05$, Online Figure VIE) whereas activation properties were unchanged (Online Figure VIE-F). We next used CASK sh-RNA plasmid with the RFP reporter (shCASK) to transfect HEK293-$Na_V1.5$; scramble shRNA with RFP was used as control (shscr). CASK protein level was decreased by 45% in shCASK at 5 D*IV* (Online Figure VIB-C). Voltage clamp experiments showed a significant increase in I_{Na} density at several tested voltages in shCASK-transfected cells (Online Figure VIG). Steady-state

inactivation was ~6 mV more positive in shCASK cells (P<0.01) whereas no difference was found for activation properties between groups (Online Figure VIH-I).

These results confirmed that CASK is excluded from ID structures and established that the negative regulatory function of CASK is a conserved mechanism.

The regulatory function of CASK is conserved in myocytes from CASK knockdown mouse.

To assess the functional regulation of sodium channels by CASK *in vivo*, I_{Na} was recorded in freshly isolated ventricular myocytes from αMHC-Cre/CASK and αMHC-Cre/WT mice. The homozygous floxed CASK^{tm1Sud} mouse was bred with a α myosin heavy chain (αMHC)-Cre mouse to target cardiomyocytes. Recombination with αMHC-Cre leads to 68% CASK knockdown (KD) in cardiomyocytes (p<0.01, N=3, Figure 5A). The incomplete extinction of CASK is likely due to contamination by non-myocyte cells. Average I-V plots from voltage clamp experiments showed a significant increase in I_{Na} density at several tested voltages in CASK KD compared with WT Cre myocytes (Figure 5B-C). No significant differences were found for activation properties and steady-state inactivation between CASK KD and WT Cre mouse myocytes (Figure 5D-E).

The results obtained in CASK KD ventricular myocytes together with the results obtained in HEK293-$Na_V1.5$ and cultured atrial myocytes support that CASK-induced effect is not dependent on the experimental model used nor on atrial versus ventricular myocytes.

CASK affects trafficking of $Na_V1.5$.

Since I_{Na} was regulated by CASK expression level, we dissected out the mechanisms of $Na_V1.5$ regulation.

RT-qPCR experiments were performed to investigate whether CASK influenced the expression level of *scn5a*. However, the copy number of *scn5a* was not different between controls and CASK-overexpressing or CASK-silenced myocytes (Figure 6A). Western blots performed form lysates of Ad-shscr and Ad-shCASK infected atrial myocytes revealed that $Na_V1.5$ protein expression was not modified by CASK silencing. Interestingly, CASK silencing impacted syntrophin level, reducing its expression by 34% (p<0.001), whereas dystrophin levels remained unchanged (Online Figure VII). Biotinylation experiments were performed to assess $Na_V1.5$ surface expression. In Ad-shCASK myocytes, $Na_V1.5$ expression was reduced by ~20% in the total fraction whereas increased by ~45% in the membrane fraction (P<0.05, Figure 6B). TIRFm experiments also demonstrated a ~20% increase in surface staining of $Na_V1.5$ in Ad-shCASK myocytes (P<0.001, Figure 6C). These results showed that the increase in I_{Na} upon CASK silencing was nor transcriptional nor translational and rather due to increased surface expression of $Na_V1.5$. Therefore, a likely explanation was that CASK regulates anterograde trafficking and/or stabilization at the sarcolemma.

As the canonical early step in ion channel trafficking is the transport from the endoplasmic reticulum (ER) to the Golgi apparatus, the hypothesis of an increased forward trafficking was tested in silencing conditions. 12h post-infection with Ad-shscr or Ad-shCASK, cardiomyocytes were treated for 48h with brefeldin-A (BFA) prior to electrophysiological recordings. Voltage-clamp experiments showed that I_{Na} density was not increased in Ad-shCASK-infected cells after BFA treatment (Figure 6D). TIRFm experiments also showed a reduced $Na_V1.5$ surface staining in Ad-shCASK myocytes treated with BFA (Figure 6E). In addition, biotinylation experiments performed on HEK293-$Na_V1.5$ cells showed that the increase in $Na_V1.5$ surface expression was reduced after BFA treatment in shCASK cells (Figure 6F).

Therefore, these results indicate that alterations in trafficking processes are involved in the effect of CASK in the regulation of I_{Na}.

CASK silencing modulates the expression of $Na_V1.5$ channels at the lateral membrane.

To understand further the mechanisms of $Na_V1.5$ regulation by CASK, we investigated whether CASK silencing affected a specific $Na_V1.5$ channel population.

Ad-shscr or Ad-shCASK infected atrial myocytes were cultured at half confluence, a situation that allows formation of cell contacts (ID-like structures) between some myocytes as well as the preservation of free membranes (LM-like structures) (Figure 7A). Immunostainings of $Na_V1.5$ channels were performed and quantified by drawing lines in contact zones *versus* free membranes. As shown Figure 7B, the $Na_V1.5$ signal was increased by ~21% at LM ($p<0.01$) and by ~10% at ID (not significant) in CASK-silenced myocytes (Figure 7B). These results support that the LM membrane pool of $Na_V1.5$ channels is more susceptible to CASK modulation. In addition, it supports the concept that different $Na_V1.5$ pools co-exist in cardiomyocytes.

CASK expression is downregulated in remodeled atria whereas its localization is unchanged.

Given the specific targeting of CASK to the costamere, we examined whether the expression and localization of the protein could be altered during conditions characterized by the remodeling of myocardial structure and of myocyte architecture such as dilated atria[18,20,21].

In control human atrial tissue samples, CASK was expressed at the LM and excluded from ID as in rat (Figure 8A). In patients with dilated atria, CASK remained localized at the costamere whereas its expression level was reduced as evidenced by fainter fluorescence intensity ($p<0.001$, Figure 8B) and a by ~42% decrease in total protein expression ($p<0.01$, Figure 8C). Chronically hemodynamic atrial overload associated with the development of ischemic heart failure in rat is also characterized by profound ultrastructural alterations of atrial myocytes[18,20]. In this model too, CASK protein expression was decreased whereas its localization in membrane subdomains remained unchanged (Online Figure VIII). These results indicate that CASK expression in downregulated during atrial remodeling.

DISCUSSION

This study is the first characterization of CASK in cardiomyocytes. We found that CASK is the sole cardiac MAGUK protein identified so far excluded from the ID and strictly located at LM, where it associated with dystrophin. We showed that CASK directly interacts with $Na_V1.5$ C-terminus and downregulates the sodium current. CASK silencing decreases syntrophin protein levels without impacting $Na_V1.5$ or dystrophin expression levels. We demonstrated that CASK modulates the early trafficking of $Na_V1.5$ and prevents its functional expression at the cell surface, and more specifically at the lateral membrane. Finally, we showed that CASK expression is reduced during atrial remodeling but its localization unchanged.

Unique localization of CASK in cardiomyocytes.

The two already known cardiac MAGUK proteins, SAP97 and ZO-1, are both preferentially expressed at the ID, a membrane domain specialized in the rapid propagation of action potentials (AP) along cardiac fibers. ID, located at the ends of cardiomyocytes, are the sites of intense electrical activity and concentrate numbers of ion channels, notably the main cardiac sodium channel, $Na_V1.5$. It has been proposed that this organization facilitates longitudinal propagation of the AP over transverse propagation and determines conduction velocity (CV)[22].

$Na_V1.5$ channels located at the ID are associated with different partners such as connexin-43[2], plakophilin-2[3,4], ankyrin-G[5,6], and SAP-97[7,8]. All of these partners participate in anchoring/stabilization of $Na_V1.5$ at the ID. In accordance, the sodium current recorded by macro-patch in the midsection of cardiomyocytes (LM) is of smaller amplitude than the current recorded at the ID[23–25]. At the LM, $Na_V1.5$ has been shown to interact with the dystrophin/syntrophin complex[19]. In the dystrophin-deficient mdx mouse model of Duchenne muscular dystrophy, the LM pool of $Na_V1.5$ is strongly reduced and I_{Na} is decreased by ~30%[8,19]. In agreement, transverse CV is more reduced than longitudinal CV in ΔSIV mouse hearts[25]. From these observations, a scheme can be drawn concerning the relative contribution of the populations of $Na_V1.5$ in the propagation of the AP: the ID pool having a higher weight

than the LM pool. Our results indicate that CASK could participate in the maintenance of low level of functional $Na_V1.5$ at the LM.

CASK, a new member of the dystrophin-glycoprotein/$Na_V1.5$ macromolecular complex.
Scanning ion conductance microscopy (SICm) identified three topographic entities in the LM: T-tubules, crests and z-grooves, the latter corresponding to T-tubule openings[26]. Like T-tubules, crests show a periodicity of ~2 µm[27]. Here, we focused on the LM distribution of CASK into microdomains using high resolution 3-D deconvolution microscopy. We showed that CASK was in closer association with dystrophin than with vinculin, two costameric proteins. In addition, we showed that CASK was able to precipitate dystrophin and that CASK staining at LM was extinct in mdx cardiomyocytes, suggesting that dystrophin is necessary for proper localization of CASK. However, in contrast to dystrophin which also extends along T-tubules in the rat myocardium, CASK was not found deep in the T-tubule since it did not colocalize with calcium channels or ryanodine receptors and its expression pattern was not affected by detubulation.

Interestingly, we showed that CASK silencing reduced syntrophin levels, whereas dystrophin and $Na_V1.5$ levels were unchanged. In addition, we showed that CASK directly interacts with the $Na_V1.5$ channel C-terminus using myocyte enriched fraction from rat heart lysates. Moreover, $Na_V1.5$ C-terminus also interacted with purified CASK protein, suggesting that $Na_V1.5$ and CASK interaction is not dependent on the presence of syntrophin. Altogether, these results suggest that CASK is downstream dystrophin and upstream syntrophin and that syntrophin and CASK could compete for $Na_V1.5$ channel binding, likely at early stages of trafficking.

Super-resolution scanning patch-clamp recordings showed that $Na_V1.5$ channels do not distribute homogenously along the LM but instead form clusters confined into functional microdomains, with the largest aggregated at crest regions[27]. Here, we showed that CASK, $Na_V1.5$ and dystrophin all displayed a periodicity of 2 µm and that CASK was associated with $Na_V1.5$. In light of this distribution and poor expression in T-tubules, one could speculate that the macromolecular complex formed by $Na_V1.5$, CASK and dystrophin corresponds to crest structures identified by SICm. The differential distribution of $Na_V1.5$ in microdomains of the LM suggests distinct roles for crests and T-tubules in electrical and contractile activities of cardiomyocytes. For instance, $Na_V1.5$ located at the crest could play a preferential role in the propagation of the action potential along the LM whereas those located in T-tubules could be involved in EC coupling. In this line, the specific localization of CASK at LM and its exclusion from T-tubules suggests a role for CASK in the regulation of the surface pool/crest population of sodium channels.

Mechanisms of regulation of I_{Na} by CASK.
MAGUKs are multidomain scaffolding proteins known to be involved in trafficking, targeting, and signaling of ion channels and receptors. In neurons, differential sorting of glutamate receptor subtypes has been shown to start in the endoplasmic reticulum (ER) and to depend on SAP97 and CASK. While AMPARs are trafficked to the plasma membrane *via* the classical secretory pathway, NMDARs are diverted towards a specialized ER sub-compartment. This ER sub-compartment is composed of NMDAR subunits, CASK and SAP97. While CASK does not directly bind to NMDAR, it prevents the SAP97-dependent ER retention of NMDAR[28]. When bound to CASK, SAP97 colocalizes with NMDAR while, when unbound, SAP97 preferentially associates with AMPAR[29]. These studies suggest that CASK regulates SAP97 association with glutamate receptor subtypes and subsequent sorting and trafficking to correct location. In cardiomyocytes, Shy *et al.* showed that the last 3 residues of $Na_V1.5$ in C-terminal, the SIV motif, are essential for the localization of $Na_V1.5$ at the LM, but not required for its expression at the ID and t-tubules[25]. The SIV motif interacts with syntrophin at the LM and with SAP97 at the ID, thereby defining distinct pools of $Na_V1.5$ multiprotein complexes. However, the mechanisms regulating the differential sorting of $Na_V1.5$ to specific membrane subdomains have not been elucidated.

In this context, the present study provides new insights in processes regulating the sorting of $Na_V1.5$. Our results revealed that CASK exerts a repressive effect on the functional expression of $Na_V1.5$. *In vitro* silencing or *in vivo* knockdown of CASK increased I_{Na}. In addition, this negative regulatory function was conserved for both atrial and ventricular myocytes. We showed that the current increase observed following CASK-silencing was due to increased surface expression of $Na_V1.5$, and more specifically, at the LM. Treatment with the inhibitor of forward transport between ER and Golgi apparatus, BFA, prevented the effect. This result shows that CASK impedes $Na_V1.5$ trafficking. Therefore, one could hypothesizes that $Na_V1.5$ sorting could be determined during anterograde processing steps of trafficking. Despite a common biosynthetic pathway, the early association of the channel with β auxiliary subunits and/or with other partners during biosynthesis could determine its sorting and final targeting to specific subdomains. Our results support that CASK plays a role in maintaining low level of $Na_V1.5$ at the LM by repressing a yet unknown identified step of channel trafficking. In this regard, CASK is unique among MAGUK proteins investigated so far that usually favors anchoring/stabilization of ion channels at the sarcolemma.

CASK expression is reduced during atrial remodeling.

Costameres encircle myocytes perpendicularly to their longitudinal axis in alignment with z-lines, making the bridge between extracellular matrix, sarcolemma and intracellular contractile sarcomeres. They reinforce the sarcolemma during cardiac workload and transmit contractile forces exerted by myocytes or extracellular matrix in a bidirectional manner[30].

Both in human and rat diseased atria characterized by extensive structural alterations of atrial myocytes[20], CASK expression levels was reduced whereas its LM localization was not modified. Whether this downregulation of CASK is associated with the redistribution of NaV1.5 subpopulations in diseased myocardium needs to be carefully examined.

In summary, this study constitutes the first description of an unconventional MAGUK protein both in terms of localization and function in the heart. CASK acts as a repressor of the population of $Na_V1.5$ dedicated to the LM by preventing early trafficking. These results represent a substantial step forward in the concept of differentially regulated pools of $Na_V1.5$ within the cardiomyocyte having distinct roles in cardiac physiology. Notably, CASK could participate in maintaining low level of $Na_V1.5$ at the lateral membrane and consequently, contribute to the anisotropic conduction.

ACKNOWLEDGMENTS

We thank Dr. H. Boycott for careful reading of the manuscript and helpful comments. We acknowledge the contribution of S. Vermij in acquiring data and preparing material for the Figs. 3 and 5. We thank M. Essers (Dpt. of Clinical Research, University of Bern, Switzerland) for kindly providing the mdx mouse heart samples. We thank Dr. N. Mougenot of PECMV Platform, Pitié-Salpêtrière Hospital, France, for helpful assistance with the animal model.

SOURCE OF FUNDING

This work was supported by Fondation Leducq "Structural Alterations in the Myocardium and the Substrate for Cardiac Fibrillation" (EB and SNH), the European Union (EUTRAF-261057; EB and SNH), and the AFM-Telethon with the reference 17758 (EB), and the Swiss National Science Foundation (grant #310030_165741, HA).

DISCLOSURES

None.

REFERENCES

1. Balse E, Steele DF, Abriel H, Coulombe A, Fedida D, Hatem SN. Dynamic of ion channel expression at the plasma membrane of cardiomyocytes. *Physiol Rev*. 2012;92:1317–58.
2. Agullo-Pascual E, Lin X, Leo-Macias A, Zhang M, Liang F-X, Li Z, Pfenniger A, Lübkemeier I, Keegan S, Fenyö D, Willecke K, Rothenberg E, Delmar M. Super-resolution imaging reveals that loss of the C-terminus of connexin43 limits microtubule plus-end capture and NaV1.5 localization at the intercalated disc. *Cardiovasc Res*. 2014;104:371–381.
3. Sato PY, Musa H, Coombs W, Guerrero-Serna G, Patiño GA, Taffet SM, Isom LL, Delmar M. Loss of plakophilin-2 expression leads to decreased sodium current and slower conduction velocity in cultured cardiac myocytes. *Circ Res*. 2009;105:523–526.
4. Sato PY, Coombs W, Lin X, Nekrasova O, Green KJ, Isom LL, Taffet SM, Delmar M. Interactions between ankyrin-G, Plakophilin-2, and Connexin43 at the cardiac intercalated disc. *Circ Res*. 2011;109:193–201.
5. Makara MA, Curran J, Little SC, Musa H, Polina I, Smith SA, Wright PJ, Unudurthi SD, Snyder J, Bennett V, Hund TJ, Mohler PJ. Ankyrin-G coordinates intercalated disc signaling platform to regulate cardiac excitability in vivo. *Circ Res*. 2014;115:929–938.
6. Mohler PJ, Rivolta I, Napolitano C, LeMaillet G, Lambert S, Priori SG, Bennett V. Nav1.5 E1053K mutation causing Brugada syndrome blocks binding to ankyrin-G and expression of Nav1.5 on the surface of cardiomyocytes. *Proc Natl Acad Sci U S A*. 2004;101:17533–17538.
7. Milstein ML, Musa H, Balbuena DP, Anumonwo JM, Auerbach DS, Furspan PB, Hou L, Hu B, Schumacher SM, Vaidyanathan R, Martens JR, Jalife J. Dynamic reciprocity of sodium and potassium channel expression in a macromolecular complex controls cardiac excitability and arrhythmia. *Proc Natl Acad Sci U A*. 2012;109:E2134–43.
8. Petitprez S, Zmoos AF, Ogrodnik J, Balse E, Raad N, El-Haou S, Albesa M, Bittihn P, Luther S, Lehnart SE, Hatem SN, Coulombe A, Abriel H. SAP97 and dystrophin macromolecular complexes determine two pools of cardiac sodium channels Nav1.5 in cardiomyocytes. *Circ Res*. 2011;108:294–304.
9. Funke L, Dakoji S, Bredt DS. Membrane-associated guanylate kinases regulate adhesion and plasticity at cell junctions. *Annu Rev Biochem*. 2005;74:219–45.
10. Abi-Char J, El-Haou S, Balse E, Neyroud N, Vranckx R, Coulombe A, Hatem SN. The anchoring protein SAP97 retains Kv1.5 channels in the plasma membrane of cardiac myocytes. *Am J Physiol Heart Circ Physiol*. 2008;294:H1851–61.
11. Eldstrom J, Choi WS, Steele DF, Fedida D. SAP97 increases Kv1.5 currents through an indirect N-terminal mechanism. *FEBS Lett*. 2003;547:205–11.
12. El-Haou S, Balse E, Neyroud N, Dilanian G, Gavillet B, Abriel H, Coulombe A, Jeromin A, Hatem SN. Kv4 potassium channels form a tripartite complex with the anchoring protein SAP97 and CaMKII in cardiac myocytes. *Circ Res*. 2009;104:758–69.
13. Godreau D, Vranckx R, Maguy A, Goyenvalle C, Hatem SN. Different isoforms of synapse-associated protein, SAP97, are expressed in the heart and have distinct effects on the voltage-gated K+ channel Kv1.5. *J Biol Chem*. 2003;278:47046–52.
14. Rhett JM, Jourdan J, Gourdie RG. Connexin 43 connexon to gap junction transition is regulated by zonula occludens-1. *Mol Biol Cell*. 2011;22:1516–28.
15. Hsueh YP, Wang TF, Yang FC, Sheng M. Nuclear translocation and transcription regulation by the membrane-associated guanylate kinase CASK/LIN-2. *Nature*. 2000;404:298–302.
16. Cohen AR, Woods DF, Marfatia SM, Walther Z, Chishti AH, Anderson JM. Human CASK/LIN-2 binds syndecan-2 and protein 4.1 and localizes to the basolateral membrane of epithelial cells. *J Cell Biol*. 1998;142:129–38.
17. Leonoudakis D, Conti LR, Radeke CM, McGuire LM, Vandenberg CA. A multiprotein trafficking complex composed of SAP97, CASK, Veli, and Mint1 is associated with inward rectifier Kir2 potassium channels. *J Biol Chem*. 2004;279:19051–63.

18. Boycott HE, Barbier CS, Eichel CA, Costa KD, Martins RP, Louault F, Dilanian G, Coulombe A, Hatem SN, Balse E. Shear stress triggers insertion of voltage-gated potassium channels from intracellular compartments in atrial myocytes. *Proc Natl Acad Sci U A*. 2013;110:E3955–64.
19. Gavillet B, Rougier JS, Domenighetti AA, Behar R, Boixel C, Ruchat P, Lehr HA, Pedrazzini T, Abriel H. Cardiac sodium channel Nav1.5 is regulated by a multiprotein complex composed of syntrophins and dystrophin. *Circ Res*. 2006;99:407–14.
20. Rucker-Martin C, Milliez P, Tan S, Decrouy X, Recouvreur M, Vranckx R, Delcayre C, Renaud J-F, Dunia I, Segretain D, Hatem SN. Chronic hemodynamic overload of the atria is an important factor for gap junction remodeling in human and rat hearts. *Cardiovasc Res*. 2006;72:69–79.
21. Aimé-Sempé C, Folliguet T, Rücker-Martin C, Krajewska M, Krajewska S, Heimburger M, Aubier M, Mercadier JJ, Reed JC, Hatem SN. Myocardial cell death in fibrillating and dilated human right atria. *J Am Coll Cardiol*. 1999;34:1577–1586.
22. Spach MS. Anisotropy of cardiac tissue: a major determinant of conduction? *J Cardiovasc Electrophysiol*. 1999;10:887–890.
23. Verkerk AO, van Ginneken ACG, van Veen TAB, Tan HL. Effects of heart failure on brain-type Na+ channels in rabbit ventricular myocytes. *Eur Eur Pacing Arrhythm Card Electrophysiol J Work Groups Card Pacing Arrhythm Card Cell Electrophysiol Eur Soc Cardiol*. 2007;9:571–577.
24. Lin X, Liu N, Lu J, Zhang J, Anumonwo JMB, Isom LL, Fishman GI, Delmar M. Subcellular heterogeneity of sodium current properties in adult cardiac ventricular myocytes. *Heart Rhythm Off J Heart Rhythm Soc*. 2011;8:1923–1930.
25. Shy D, Gillet L, Ogrodnik J, Albesa M, Verkerk AO, Wolswinkel R, Rougier JS, Barc J, Essers MC, Syam N, Marsman RF, van Mil AM, Rotman S, Redon R, Bezzina CR, Remme CA, Abriel H. PDZ Domain-Binding Motif Regulates Cardiomyocyte Compartment-Specific NaV1.5 Channel Expression and Function. *Circulation*. 2014;130:147–60.
26. Lab MJ, Bhargava A, Wright PT, Gorelik J. The scanning ion conductance microscope for cellular physiology. *Am J Physiol Heart Circ Physiol*. 2013;304:H1–11.
27. Bhargava A, Lin X, Novak P, Mehta K, Korchev Y, Delmar M, Gorelik J. Super-resolution scanning patch clamp reveals clustering of functional ion channels in adult ventricular myocyte. *Circ Res*. 2013;112:1112–1120.
28. Jeyifous O, Waites CL, Specht CG, Fujisawa S, Schubert M, Lin E, Marshall J, Aoki C, de Silva T, Montgomery JM, Garner CC, Green WN. SAP97 and CASK mediate sorting of N-Methyl-D-Aspartate Receptors through a novel secretory pathway. *Nat Neurosci*. 2009;12:1011–1019.
29. Lin EI, Jeyifous O, Green WN. CASK Regulates SAP97 Conformation and Its Interactions with AMPA and NMDA Receptors. *J Neurosci*. 2013;33:12067–12076.
30. Samarel AM. Focal adhesion signaling in heart failure. *Pflüg Arch Eur J Physiol*. 2014;466:1101–1111.

FIGURE LEGENDS

Figure 1. CASK is expressed at the lateral membrane of cardiomyocytes and excluded from the intercalated disc. (A) Representative western blot showing the expression of CASK in brain, atria and ventricle lysates and in myocyte and fibroblast enriched fractions. GAPDH served as loading control (N=2). (B) Histogram showing the relative ratio of CASK normalized to GAPDH in the different extracts. (C) High resolution 3-D deconvolution microscopy images and enlargements of outlined squares (right panels) obtained from ventricular tissue sections

stained with CASK and caveolin3 (top panel), N-cadherin (middle panel) and α-actinin (bottom panel).

Figure 2. CASK is a new member of the dystrophin-glycoprotein complex. (A) High resolution 3-D deconvolution microscopy images of CASK with vinculin and dystrophin in freshly isolated ventricular myocytes and enlargement of outlined squares (right panels). (B) Intensity plots for vinculin (n=6), dystrophin (n=4) and CASK (n=6) drawn from 10 µm lines along the LM. (C) Co-immunostaining images of CASK and dystrophin taken in the midsection of cardiomyocytes and corresponding intensity plots drawn from 15 µm lines (n=3). (D) Representative co-immunoprecipitation assays performed on whole heart lysates (N=4). (E) Co-immunostainings images of CASK and α-actinin (top panel) or dystrophin (bottom panel) in control (C57Bl6) and mdx mouse ventricular cryosections (n=6).

Figure 3. CASK is associated to and interacts with $Na_V1.5$ channels. (A) High resolution 3-D deconvolution microscopy images of CASK (left panel) and $Na_V1.5$ (right panel) taken from freshly isolated atrial myocytes and enlargement of outlined squares. Intensity plots for CASK and $Na_V1.5$ drawn from 12 µm lines in the midsection of the cell and interval distribution (bottom panels) (n=8). (B) Co-immunostaining of CASK and $Na_V1.5$ performed with another pair of antibodies and enlargement of outlined square. (C) Representative co-immunoprecipitation assay of CASK and $Na_V1.5$ performed on whole heart lysates (N=4). (D) Scheme of GST fusion proteins used to perform pull-down experiments. The 66 last amino acids (Ct) of WT $Na_V1.5$ or deleted for the PDZ interacting motif (SIV) were compared to GST alone. (E and F) Representative western blots following GST pull-downs performed with cardiomyocytes enriched lysates (E, N=3) or purified protein CASK (F, N=3). CASK and syntrophin both interact with $Na_V1.5$ C-terminus and a part of this interaction is mediated by the SIV motif. Ponceau stainings served as loading controls.

Figure 4. CASK regulates the cardiac sodium current I_{Na} in cultured adult atrial myocytes. (A) Family traces of whole-cell I_{Na} recorded in cardiomyocytes infected with Ad-GFP or Ad-CASK. (B) Family traces of whole-cell I_{Na} recorded in cardiomyocytes infected with Ad-shscr or Ad-shCASK. (C) Current density-voltage relationships (25 mmol/L $[Na^+]_o$) of I_{Na} obtained from Ad-GFP (black) and Ad-CASK (green) infected myocytes. (D-E) Voltage-dependent activation and steady-state inactivation curves from Ad-GFP and Ad-CASK atrial myocytes (N=3). (F) Current density-voltage relationships (25 mmol/L $[Na^+]_o$) of I_{Na} obtained from Ad-shscr (black) and Ad-shCASK (red) infected myocytes. (G-H) Activation and steady-state inactivation curves from Ad-shscr and Ad-shCASK infected myocytes (N=3). * P<0.05; ** P<0.01; *** P<0.001.

Figure 5. The cardiac sodium current I_{Na} is upregulated by CASK knockdown in mouse ventricular myocytes. (A) Representative western blot showing the reduction of CASK expression in heart lysate from CASK KO mice (N=3). (B) Family traces of whole-cell I_{Na} recorded in freshly isolated ventricular myocytes from WT Cre or CASK KO mice. (C) Current density-voltage relationships (5 mmol/L $[Na^+]_o$) of I_{Na} obtained from WT Cre (black) and CASK KO (red) freshly isolated ventricular myocytes. (D-E) Voltage-dependent activation and steady-state inactivation curves from WT Cre and CASK KO freshly isolated cardiomyocytes (N=3). * P<0.05; ** P<0.01; *** P<0.001.

Figure 6. CASK regulates early anterograde trafficking of $Na_V1.5$ channels. (A) RT-qPCR histogram of CASK mRNA expression levels in myocytes infected with Ad-GFP (black), Ad-CASK (green), Ad-shscr (black) or Ad-shCASK (red) (N=4). (B) Representative biotinylation assay performed in Ad-shscr and Ad-shCASK infected atrial myocytes and corresponding histogram showing the expression level of $Na_V1.5$ normalized to GAPDH in total and surface fractions (N=3). (C) Example TIRFm images taken from fixed Ad-shscr (black) and Ad-shCASK (red) atrial myocytes and corresponding histogram of $Na_V1.5$ evanescent field fluorescence

(EFF) intensity (arbitrary units, AU). (D) Current density-voltage relationships (25 mmol/L $[Na^+]_o$) of I_{Na} obtained from adult atrial myocytes infected with Ad-shscr (black) or Ad-shCASK treated with brefeldin-A (BFA) (purple) or non-treated (red) (N=3). (E) Histogram of $Na_V1.5$ EFF intensity from TIRFm images taken from fixed atrial myocytes infected with Ad-shscr (black), Ad-shCASK treated with BFA (purple) and non-treated (red) (N=3). (F) Representative biotinylation assay performed in shscr and shCASK transfected HEK-$Na_V1.5$ cells and corresponding histogram showing the expression level of $Na_V1.5$ normalized to GAPDH in total and surface fractions (N=3). * P<0.05; ** P<0.01; *** P<0.001; ns not significant.

Figure 7. CASK silencing increases $Na_V1.5$ channels expression at the LM. (A) High resolution 3-D deconvolution microscopy images of $Na_V1.5$ in cultured atrial myocytes infected with either Ad-shscr or Ad-shCASK and enlargement of outlined squares. Arrowheads point cell contacts (ID-like structures, yellow) or free membranes (LM-like structures, blue). (B) Histograms of the mean fluorescence intensity of $Na_V1.5$ signal obtained from lines drawn along the ID (yellow) or the LM (blue) as shown in the example images (left of the histograms).

Figure 8. CASK expression is reduced in dilated and remodeled atria. (A) High resolution 3-D deconvolution microscopy images of CASK (left panel), N-cadherin (middle panel) and merged image (right panel) taken from control human and dilated atria (diseased) cryosections. Arrows indicate ID. (B) Histogram of CASK fluorescence intensity in control and diseased human atria (%) (N=6). (C) Representative western blot and corresponding histogram showing the expression level of CASK normalized to GAPDH in whole lysates from control and diseased atria (N=9). ** P<0.01; *** P<0.001.

NOVELTY AND SIGNIFICANCE

What Is Known?

- Cardiac sodium channels are located in distinct membrane domains of the cardiac myocyte and interact with several partners, defining different populations of sodium channels which could play different roles in cardiac electrophysiology.

- At the intercalated disc, a high concentration of sodium channels are found in interaction with several anchoring partners where they contribute to the fast and longitudinal propagation of the action potential.

- While recent studies have identified another subpopulation of sodium channels at the lateral membrane which underlies a sodium current of small amplitude, the partners and mechanisms regulating this subpopulation are still largely unknown.

What New Information Does This Article Contribute?

- In atrial and ventricular myocardium, we identified a new MAGUK protein, CASK, which is restricted to the lateral membrane of cardiomyocytes and interacts with both the dystrophin-glycoprotein complex and sodium channels, defining a new multi-molecular complex in this specific membrane domain.

- CASK negatively regulates the sodium current both *in vitro* and *in vivo* and reduces the surface expression of sodium channel at the lateral membrane by impeding channel trafficking.

- CASK appears as a crucial determinant of the organization of the subpopulation of sodium channel of the lateral membrane; its reduced expression in diseased myocardium might contribute to the alteration of the normal anisotropic propagation of the electrical influx.

Cardiomyocytes are highly organized cells characterized by specific plasma membrane domains specialized in mechanical and electrical functions. These domains are constituted by macromolecular complexes containing several ion channels and partners, particularly well described for the intercalated disc. Here, we describe a new macromolecular complex at the lateral membrane of cardiomyocytes which organizes a subpopulation of sodium channels. We found that the MAGUK protein CASK is an unconventional partner of $Na_V1.5$ channels in cardiomyocytes. CASK is specifically distributed in costameric structures of the lateral membrane in association with dystrophin. We show that CASK directly interacts with $Na_V1.5$ and negatively regulates the corresponding current both *in vitro* and *in vivo* and impedes $Na_V1.5$ trafficking to the plasma membrane. Finally, we show that CASK expression is reduced in remodeled/dilated atrial biopsies without changes in localization. These results not only strengthen the concept of differentially regulated pools of $Na_V1.5$ channels within the cardiomyocyte but also suggest that CASK could participate in maintaining low levels of active $Na_V1.5$ at the lateral membrane. Given the role of $Na_V1.5$ in the fast activation and propagation of the action potential, the repressive effect of CASK on $Na_V1.5$ could contribute to the anisotropic conduction of the depolarization wave.

Figure 1

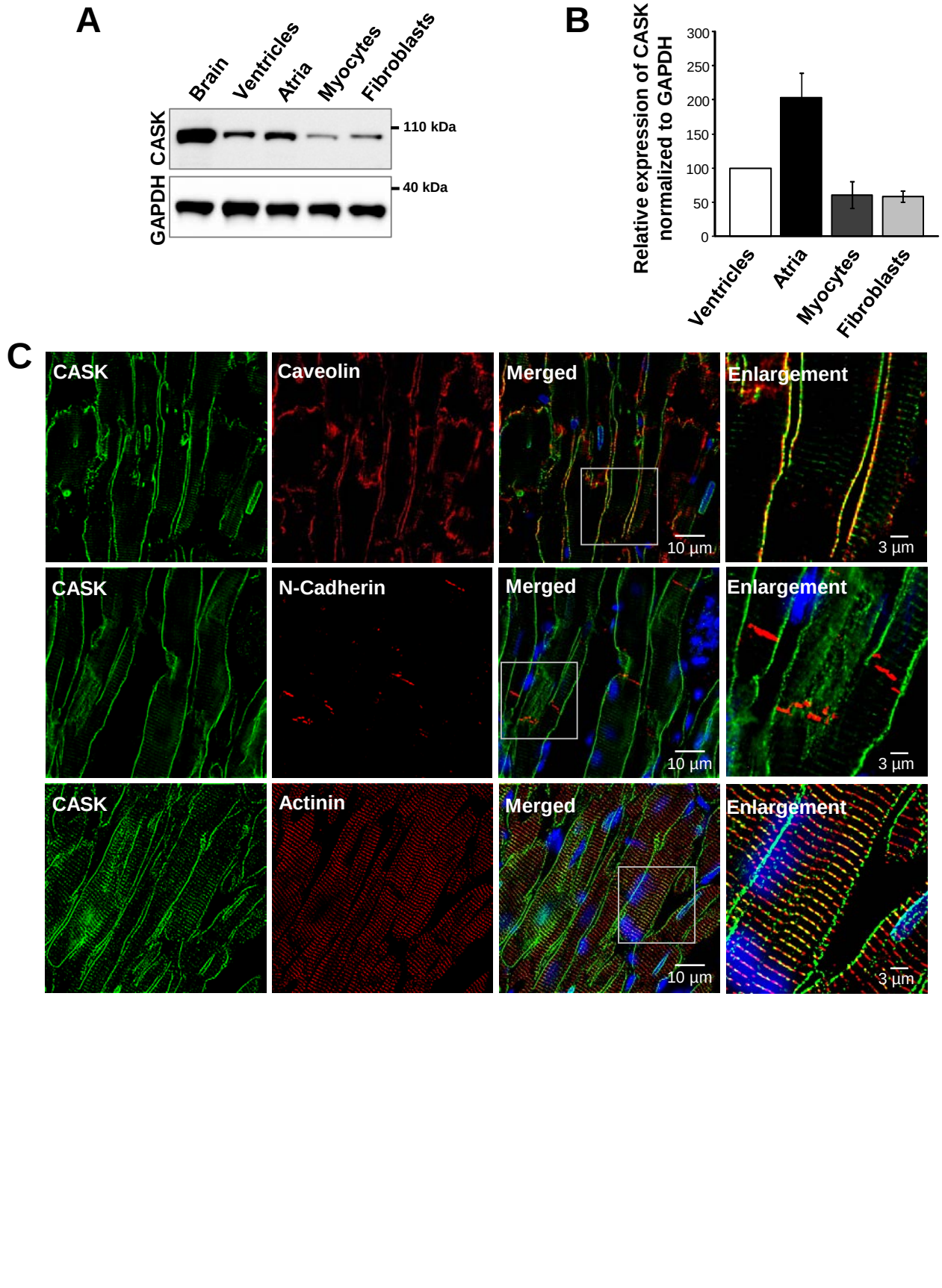
A
Brain
Ventricles
Atria
Myocytes
Fibroblasts
CASK
GAPDH
110 kDa
40 kDa
B
Relative expression of CASK normalized to GAPDH
300
250
200
150
100
50
0
Ventricles
Atria
Myocytes
Fibroblasts
C
CASK
Caveolin
Merged
Enlargement
10 µm
3 µm
CASK
N-Cadherin
Merged
Enlargement
10 µm
3 µm
CASK
Actinin
Merged
Enlargement
10 µm
3 µm

Figure 2

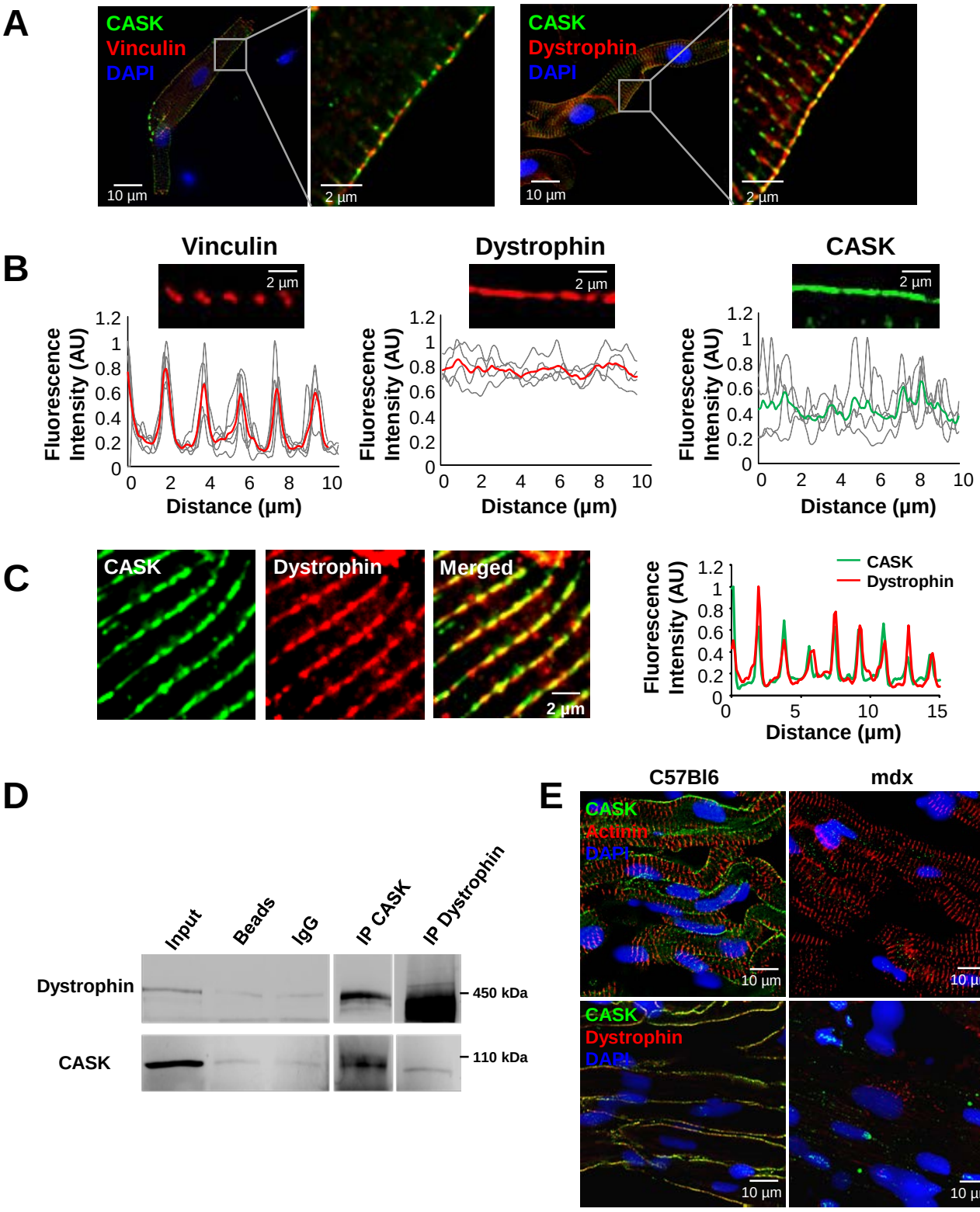
A
CASK
Vinculin
DAPI
10 µm
2 µm
CASK
Dystrophin
DAPI
10 µm
2 µm
B
Vinculin
Dystrophin
CASK
2 µm
Fluorescence Intensity (AU)
Distance (µm)
C
CASK
Dystrophin
Merged
2 µm
Fluorescence Intensity (AU)
Distance (µm)
D
Input
Beads
IgG
IP CASK
IP Dystrophin
Dystrophin
CASK
450 kDa
110 kDa
E
C57Bl6
mdx
CASK
Actinin
DAPI
CASK
Dystrophin
DAPI
10 µm

Figure 3

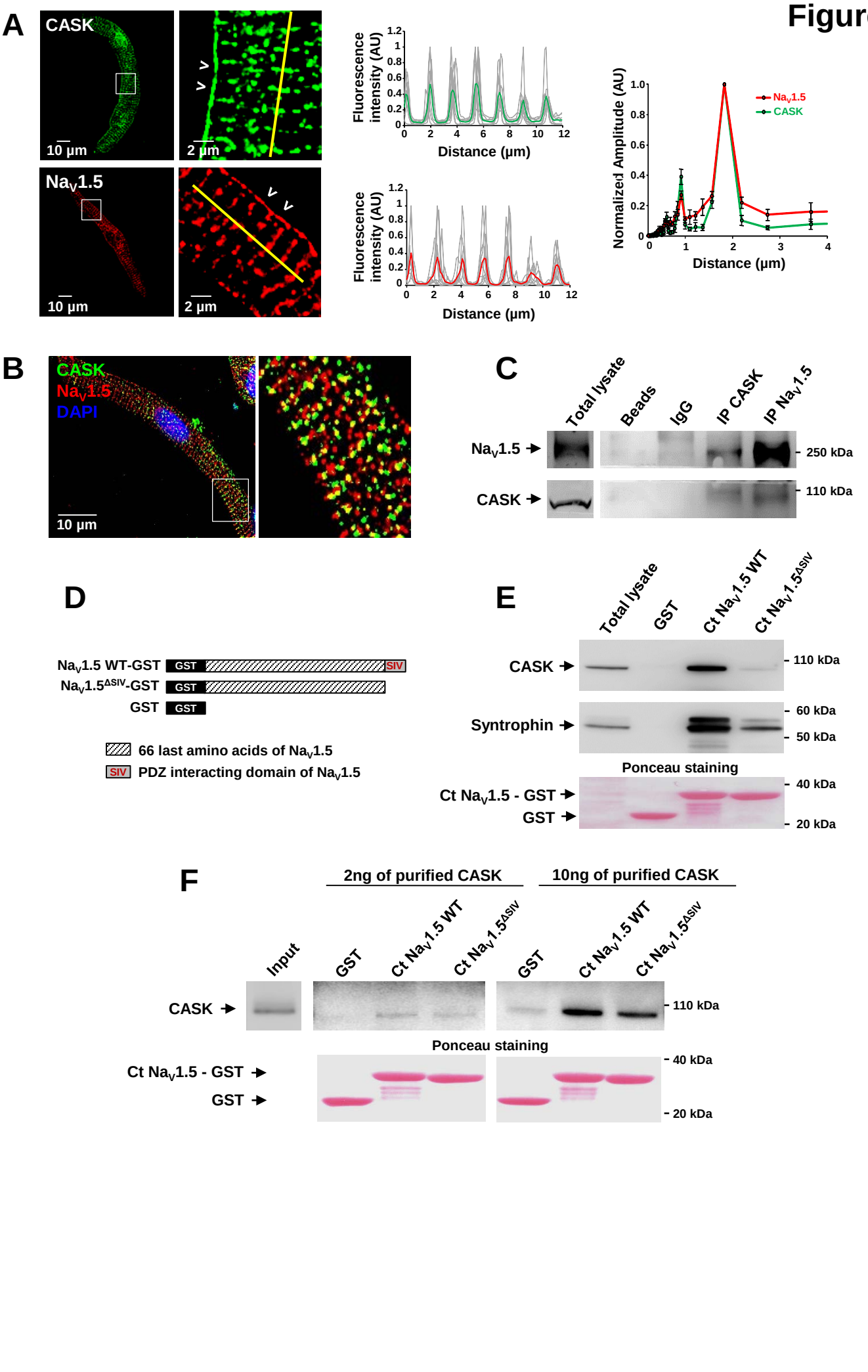
A
CASK
10 µm
2 µm
Na$_V$1.5
10 µm
2 µm
Fluorescence intensity (AU)
Distance (µm)
Fluorescence intensity (AU)
Distance (µm)
Normalized Amplitude (AU)
Na$_V$1.5
CASK
Distance (µm)
B
CASK
Na$_V$1.5
DAPI
10 µm
C
Total lysate
Beads
IgG
IP CASK
IP Na$_V$1.5
Na$_V$1.5
250 kDa
CASK
110 kDa
D
Na$_V$1.5 WT-GST
GST
SIV
Na$_V$1.5$^{\Delta SIV}$-GST
GST
GST
66 last amino acids of Na$_V$1.5
SIV PDZ interacting domain of Na$_V$1.5
E
Total lysate
GST
Ct Na$_V$1.5 WT
Ct Na$_V$1.5$^{\Delta SIV}$
CASK
110 kDa
Syntrophin
60 kDa
50 kDa
Ponceau staining
Ct Na$_V$1.5 - GST
40 kDa
GST
20 kDa
F
2ng of purified CASK
10ng of purified CASK
Input
GST
Ct Na$_V$1.5 WT
Ct Na$_V$1.5$^{\Delta SIV}$
GST
Ct Na$_V$1.5 WT
Ct Na$_V$1.5$^{\Delta SIV}$
CASK
110 kDa
Ponceau staining
Ct Na$_V$1.5 - GST
40 kDa
GST
20 kDa

Figure 4

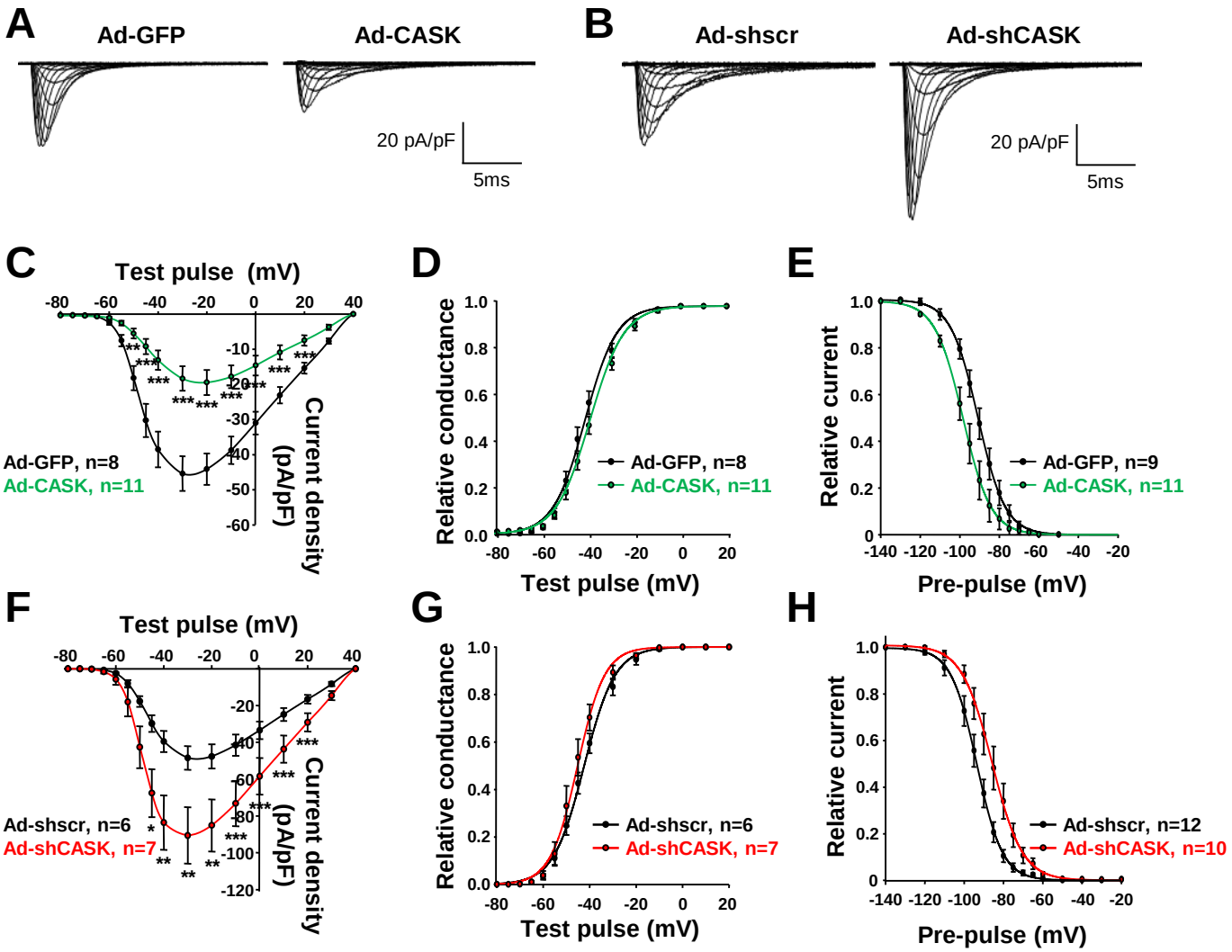
A
Ad-GFP
Ad-CASK
20 pA/pF
5ms
B
Ad-shscr
Ad-shCASK
20 pA/pF
5ms
C
Test pulse (mV)
Current density (pA/pF)
Ad-GFP, n=8
Ad-CASK, n=11
D
Relative conductance
Test pulse (mV)
Ad-GFP, n=8
Ad-CASK, n=11
E
Relative current
Pre-pulse (mV)
Ad-GFP, n=9
Ad-CASK, n=11
F
Test pulse (mV)
Current density (pA/pF)
Ad-shscr, n=6
Ad-shCASK, n=7
G
Relative conductance
Test pulse (mV)
Ad-shscr, n=6
Ad-shCASK, n=7
H
Relative current
Pre-pulse (mV)
Ad-shscr, n=12
Ad-shCASK, n=10

Figure 5

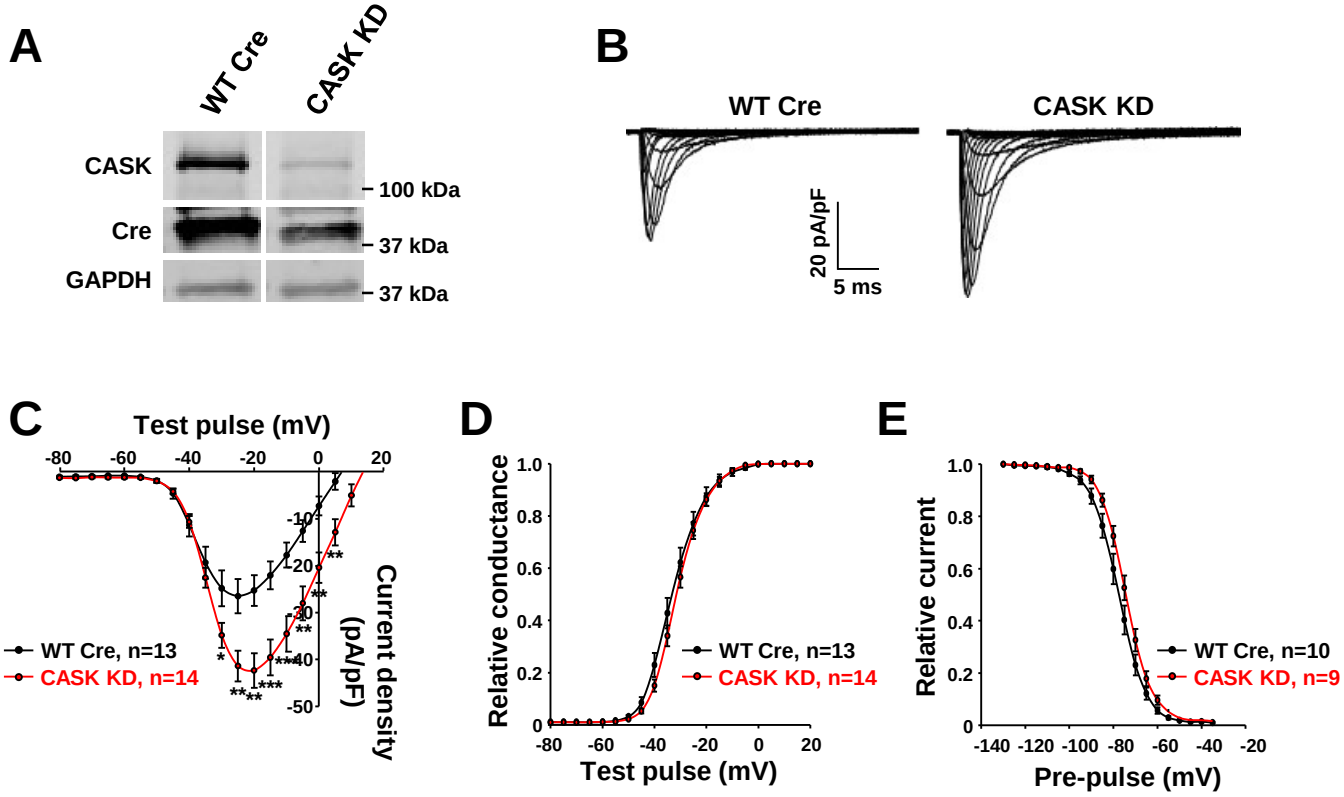
A
WT Cre
CASK KD
CASK
Cre
GAPDH
100 kDa
37 kDa
37 kDa
B
WT Cre
CASK KD
20 pA/pF
5 ms
C
Test pulse (mV)
-80 -60 -40 -20 0 20
-10 -20 -30 -40 -50
Current density (pA/pF)
WT Cre, n=13
CASK KD, n=14
D
Relative conductance
1.0 0.8 0.6 0.4 0.2 0
-80 -60 -40 -20 0 20
Test pulse (mV)
WT Cre, n=13
CASK KD, n=14
E
Relative current
1.0 0.8 0.6 0.4 0.2 0
-140 -120 -100 -80 -60 -40 -20
Pre-pulse (mV)
WT Cre, n=10
CASK KD, n=9

Figure 6

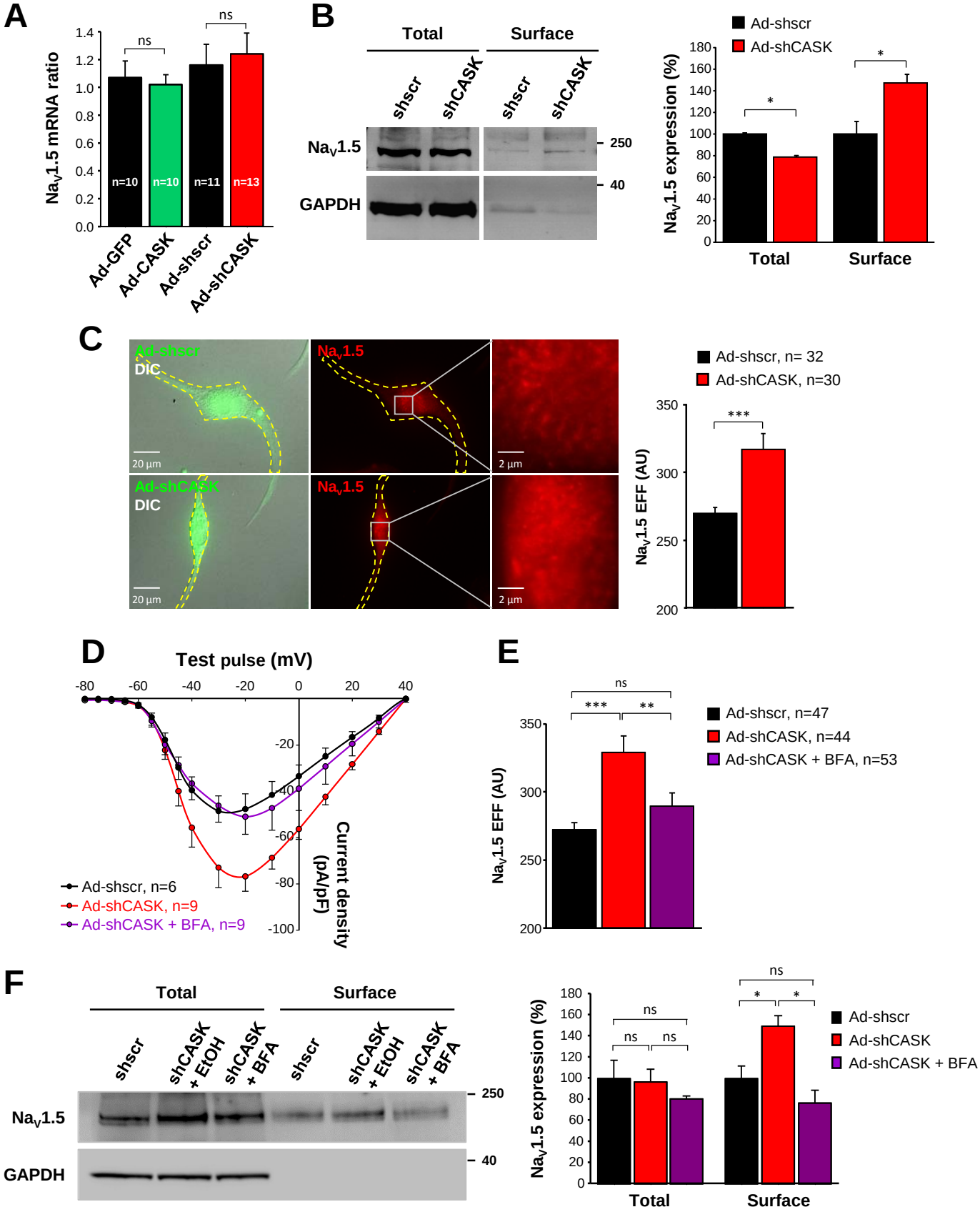
A
B
C
D
E
F
Total
Surface
shscr
shCASK
Ad-shscr
Ad-shCASK
Ad-GFP
Ad-CASK
Ad-shCASK + BFA
Ad-shscr, n= 32
Ad-shCASK, n=30
Ad-shscr, n=47
Ad-shCASK, n=44
Ad-shCASK + BFA, n=53
Ad-shscr, n=6
Ad-shCASK, n=9
Ad-shCASK + BFA, n=9
Test pulse (mV)
Current density (pA/pF)
shCASK + EtOH
shCASK + BFA
GAPDH
DIC
20 µm
2 µm
ns

Figure 7

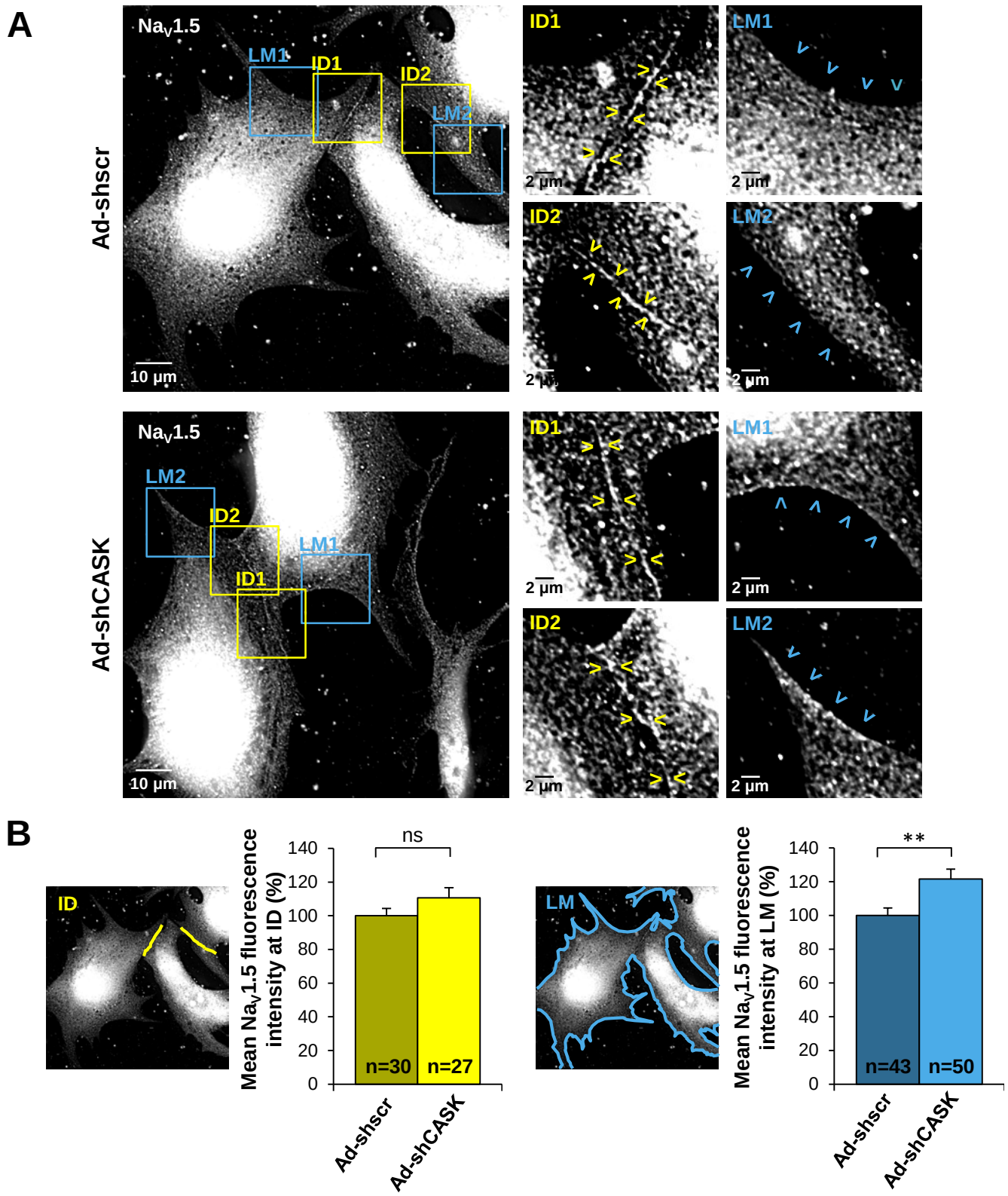
A
Ad-shscr
Ad-shCASK
Na$_V$1.5
LM1
ID1
ID2
LM2
10 µm
2 µm
B
ID
LM
Mean Na$_V$1.5 fluorescence intensity at ID (%)
Mean Na$_V$1.5 fluorescence intensity at LM (%)
ns
**
n=30
n=27
n=43
n=50
Ad-shscr
Ad-shCASK

Figure 8

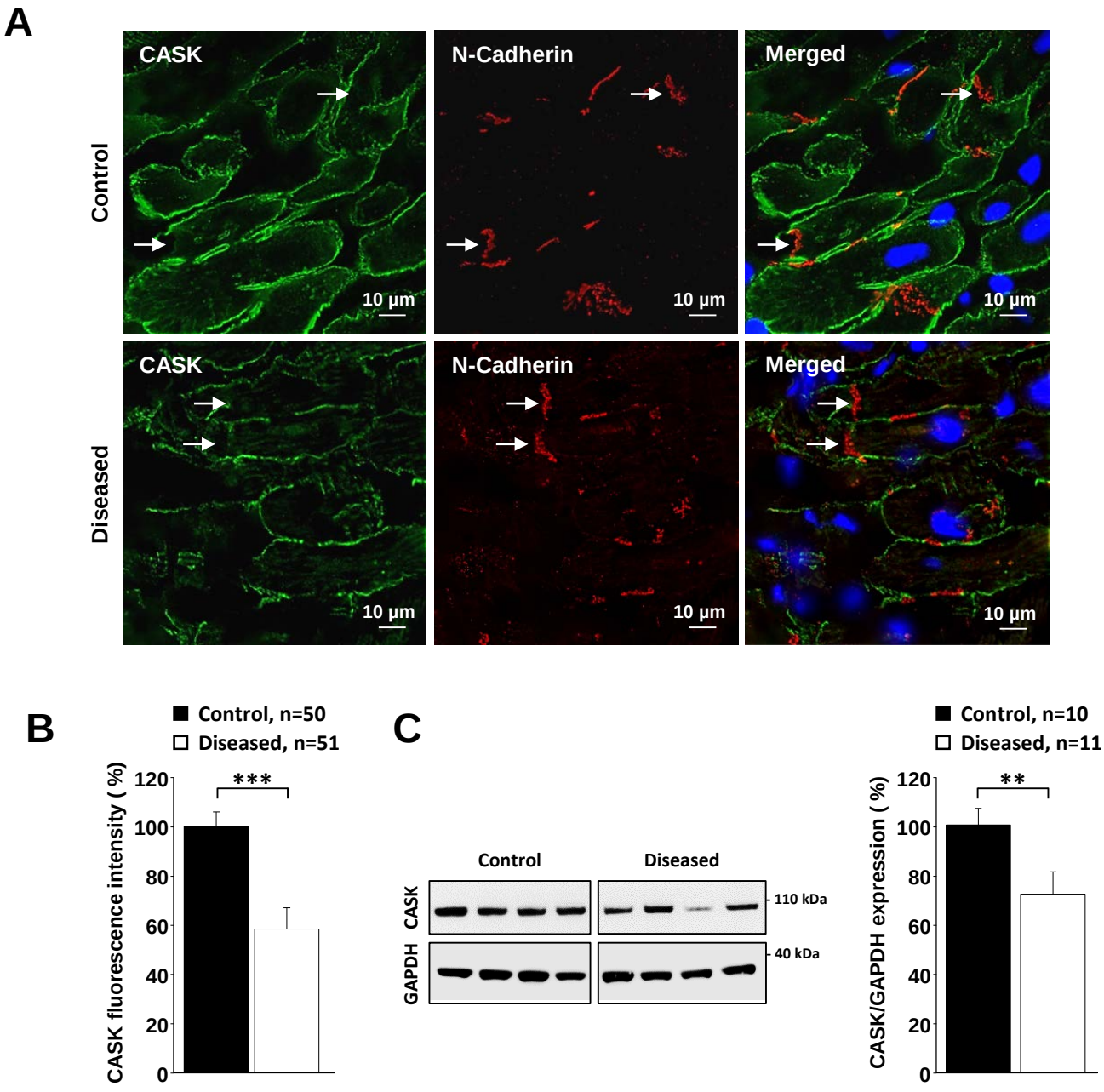
A
CASK
N-Cadherin
Merged
Control
Diseased
10 µm
B
Control, n=50
Diseased, n=51
CASK fluorescence intensity (%)
***
C
Control
Diseased
CASK
GAPDH
110 kDa
40 kDa
Control, n=10
Diseased, n=11
CASK/GAPDH expression (%)
**

Online Figure I

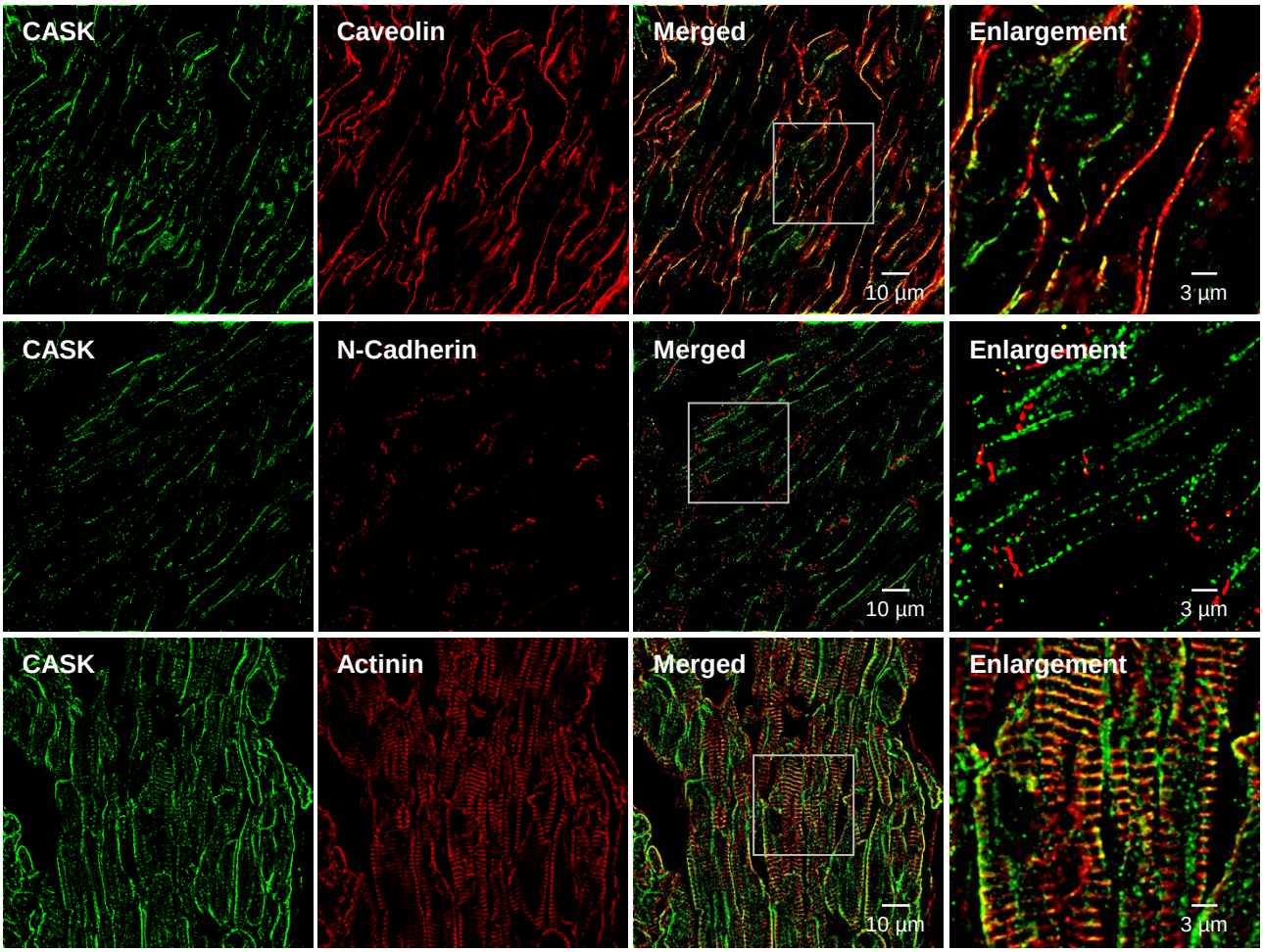

Online Figure I. CASK is expressed at the lateral membrane of cardiac myocytes and excluded from the intercalated disc in the atrial myocardium. High resolution 3-D deconvolution microscopy images and enlargements of outlined squares (right panels) obtained from atrial tissue sections stained with CASK and caveolin3 (top panel), N-cadherin (middle panel) and α-actinin (bottom panel). Note that the focal plane was selected in order to highlight the different structures of interest.

Online Figure II

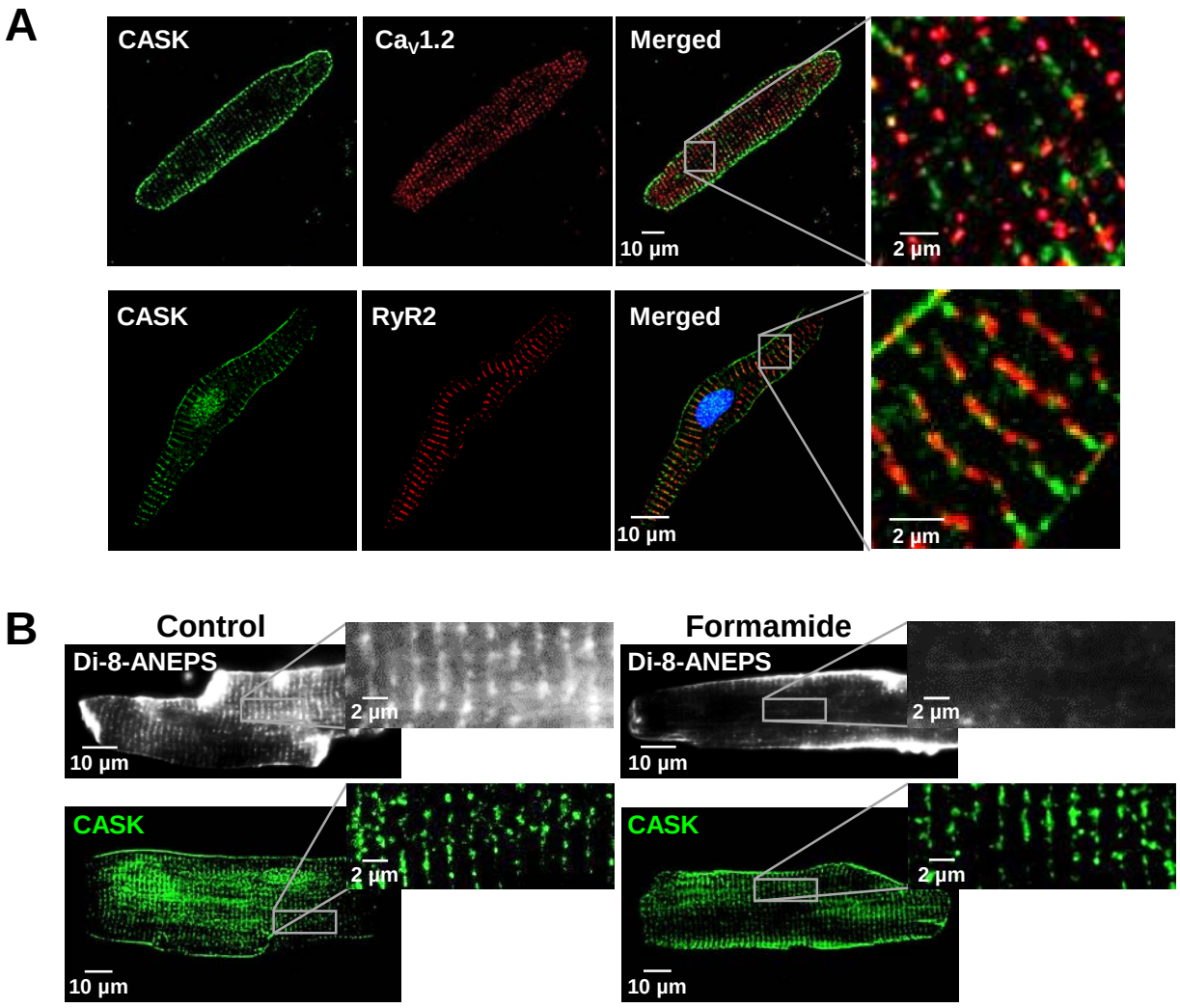

Online Figure II. CASK expression at the z-line does not correspond to T-tubule localization. (A) High resolution 3-D deconvolution microscopy images of CASK and $Ca_V1.2$ channel (top panel) or ryanodine receptor 2 (RyR2, bottom panel) in freshly isolated ventricular myocytes. Right panels correspond to enlargement of outlined squares. (B) Live images of Di-8-ANEPS staining (top panel) and post-staining of CASK after fixation (bottom panel) in control or formamide-treated cardiac myocytes.

Online Figure III

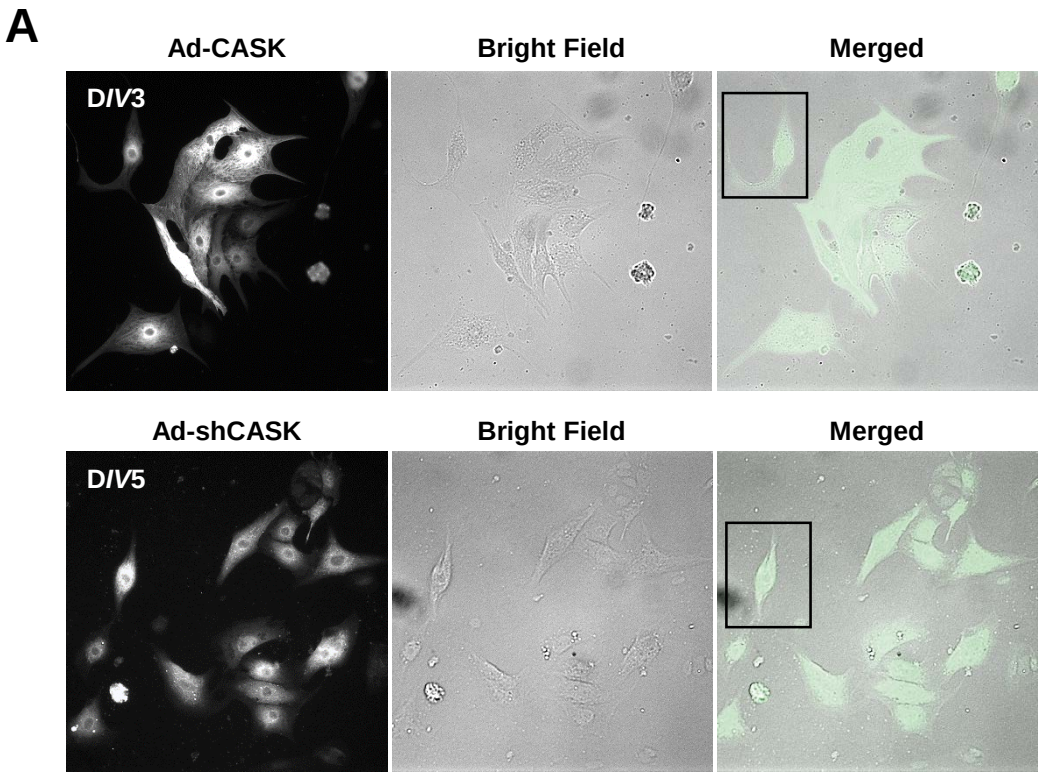

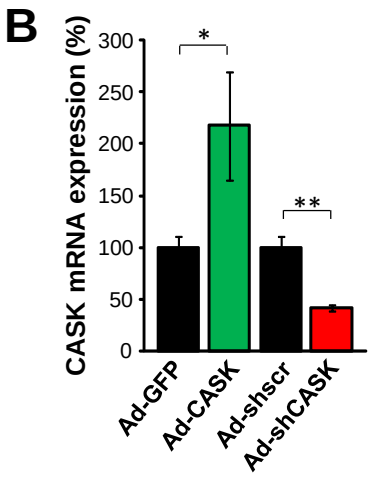

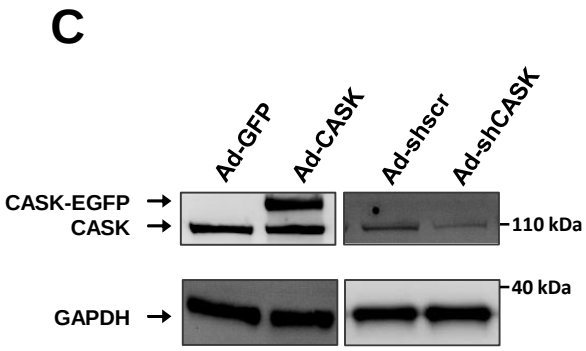

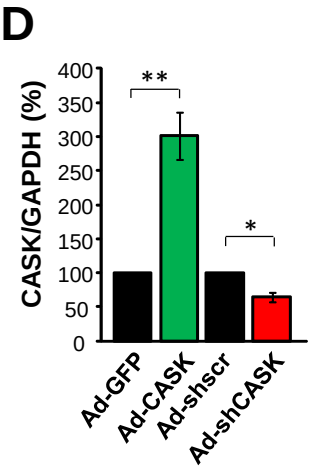

Online Figure III. Modulation of CASK mRNA and protein levels by adenoviral transfer technology. (A) Representative bright field and epifluorescence images of adenoviral infection efficiency in cultured rat atrial myocytes for overexpression (top) and silencing (bottom) experiments (20X). Squares in the merged images outline representative isolated cell used for patch clamp experiments. (B) Histogram showing the expression level of CASK mRNA in adult atrial myocytes infected with Ad-CASK (green) or Ad-shCASK (red) compared to their respective control Ad-GFP and Ad-shscr (black). (C) Representative western blot showing increased CASK expression in Ad-CASK infected myocytes (endogenous CASK at ~110 kDa and CASK-EGFP at ~140 kDa) or decreased CASK expression in myocytes infected with either Ad-shCASK. (D) Histogram of the expression level of CASK normalized to GAPDH after modulation of its expression by shRNA or overexpressing adenoviruses (N=2). * P<0.05; ** P<0.01.

Online Figure IV

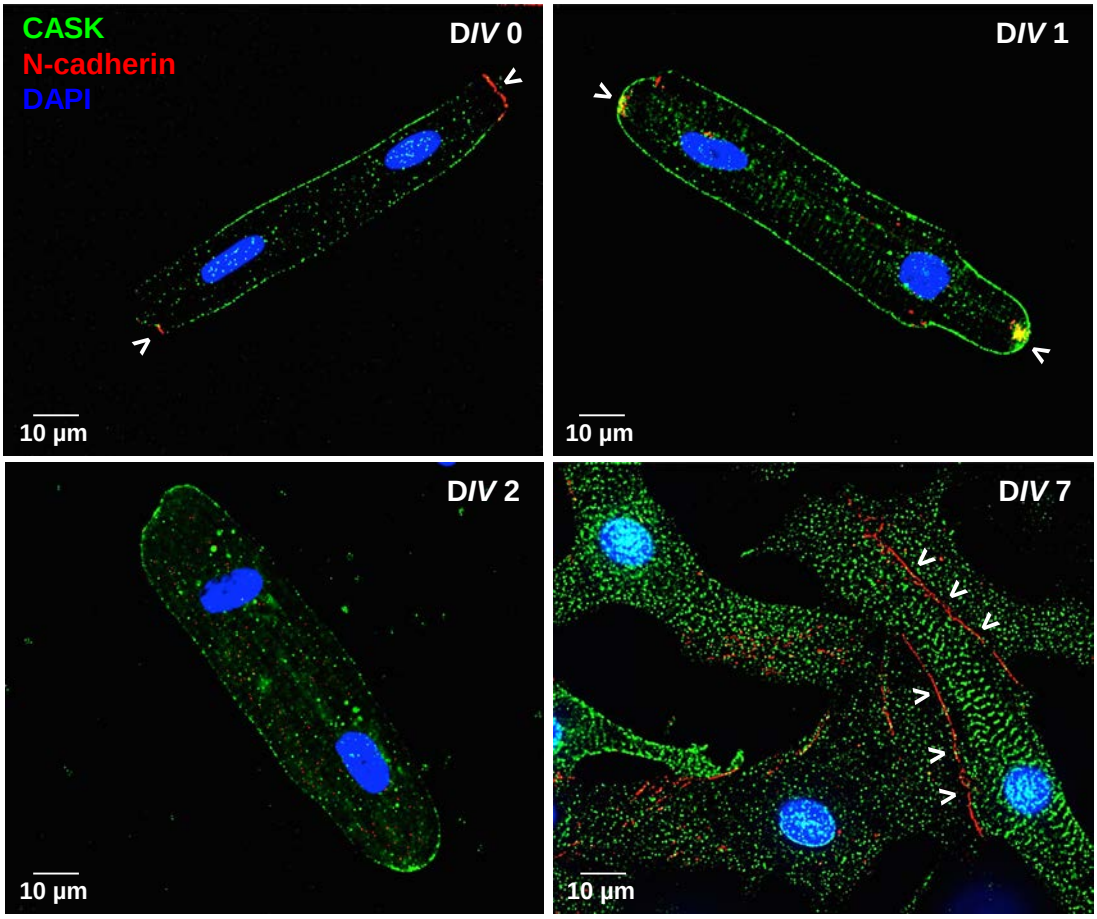

Online Figure IV. Distribution of CASK in cardiac myocytes in function of the time in culture. High resolution 3-D deconvolution microscopy images showing the distribution of CASK and the adherens junction protein N-cadherin at different days *in vitro* (D*IV*). N-cadherin was used as a marker of the intercalated disc (ID) or ID-like structures after reestablishment of cell-cell contacts. Arrowheads point the localization of ID in freshly isolated cells and cell-cell contacts stained with N-cadherin. Note that the two proteins are never associated and that CASK is absent at sites of contact.

Online Figure V

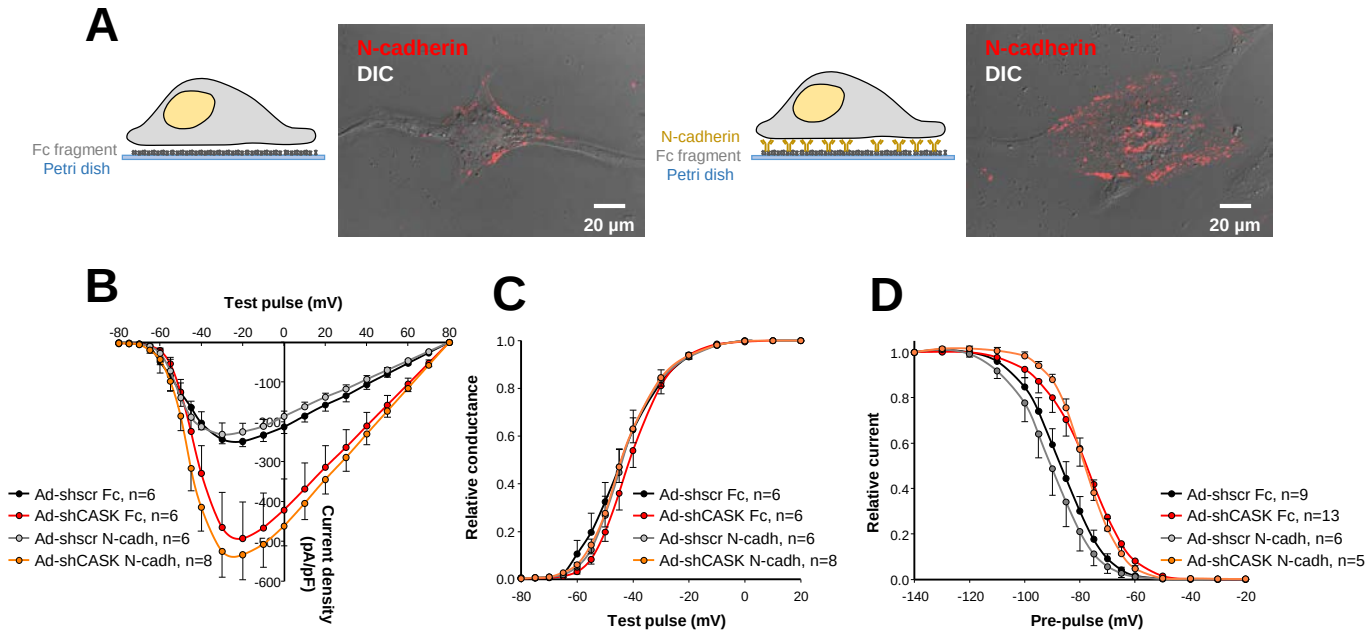

Online Figure V. CASK negatively regulates the cardiac sodium current I_{Na} in polarized cardiac myocytes. (A) Cartoon depicting the induction of adherens junctions with the substrate and corresponding TIRFm images of N-cadherin staining (right panels). (B) Current density-voltage relationships (135 mmol/L $[Na^+]_o$) of I_{Na} obtained from adult atrial myocytes infected with Ad-shscr and seeded on Fc (black) or on N-cadh (grey) or from myocytes infected with Ad-shCASK and seeded on Fc (red) or N-cadh (orange) (N=2). (C-D) Voltage-dependent activation and steady-state inactivation curves obtained from adult atrial myocytes in the same four conditions (N=2). * P<0.05; ** P<0.01; *** P<0.001.

Online Figure VI

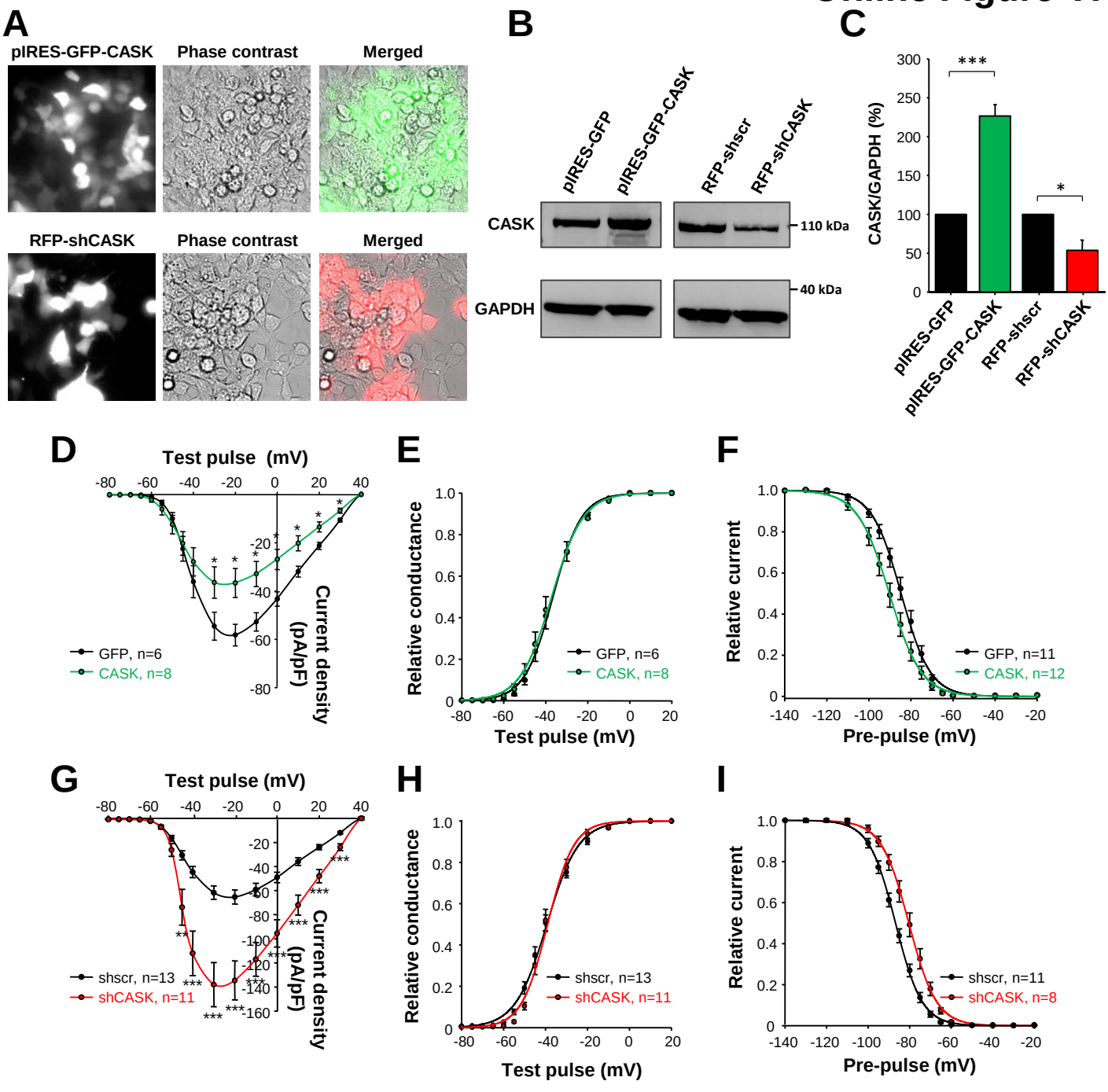

Online Figure VI. CASK regulates the cardiac sodium current I_{Na} in non-polarized HEK293-$Na_V1.5$ cells. (A) Representative phase contrast and epifluorescence images of the transfection efficiency in HEK293-$Na_V1.5$ cells. (B) Representative western blots showing CASK expression in HEK293-$Na_V1.5$ cells transfected with either pIRES-GFP-CASK or RFP-shCASK. (C) Histogram of the expression level of CASK normalized to GAPDH after modulation of its expression by overexpression plasmids or shRNA (N=2). * P<0.05; *** P<0.001. (D) Current density-voltage relationships (25 mmol/L $[Na^+]_o$) of I_{Na} obtained from GFP (black) and CASK (green) transfected HEK293 cells. (E-F) Activation and steady-state inactivation curves obtained from GFP (black) and CASK (green) HEK293 cells (N=3). (G) Current density-voltage relationships (25 mmol/L $[Na^+]_o$) of I_{Na} obtained from shscr (black) and shCASK (red) transfected HEK293 cells. (H-I) Activation and steady-state inactivation curves obtained from shscr (black) and shCASK (red) HEK293 cells (N=3). * P<0.05; ** P<0.01; *** P<0.001.

Online Figure VII

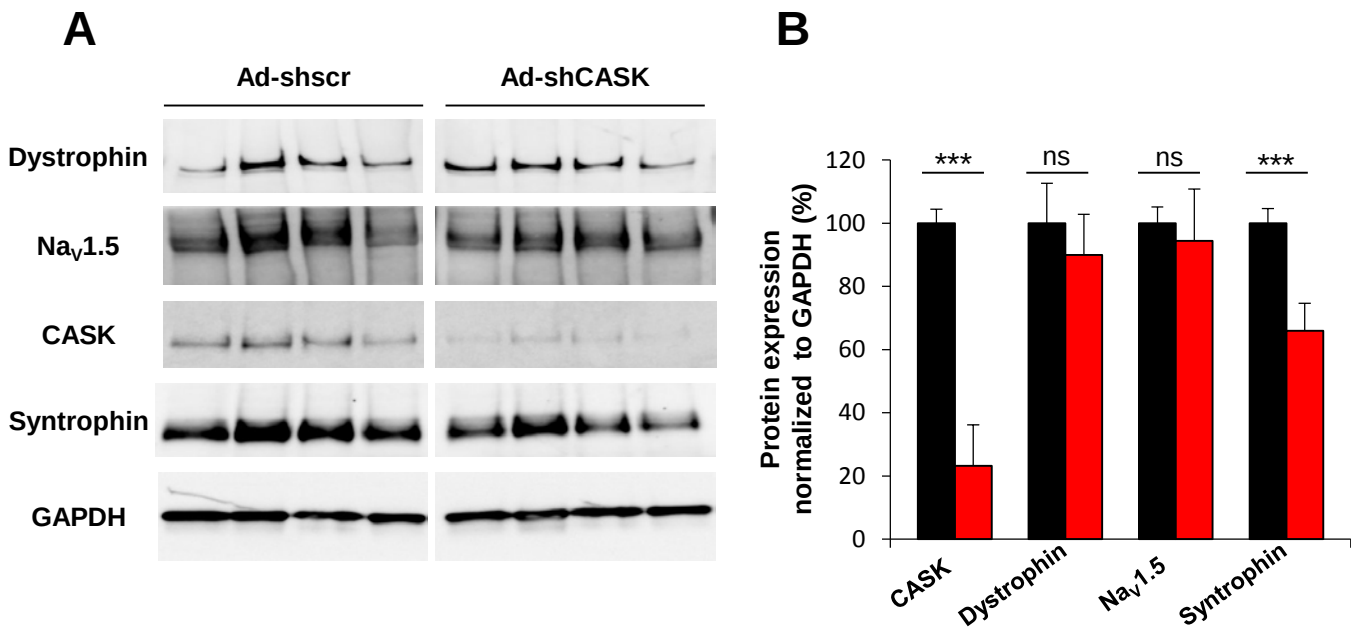

Online Figure VII. CASK silencing inhibits syntrophin expression. (A) Representative western blot showing the expression of CASK, dystrophin, $Na_V1.5$ and syntrophin in control (black) and CASK-silenced myocytes (red). GAPDH served as loading control. (B) Histogram showing the relative protein expression normalized to GAPDH in Ad-shscr and Ad-shCASK. n=7 independent cultures, N=3-5 western blots. ns, not significant; *** P<0.001.

Online Figure VIII

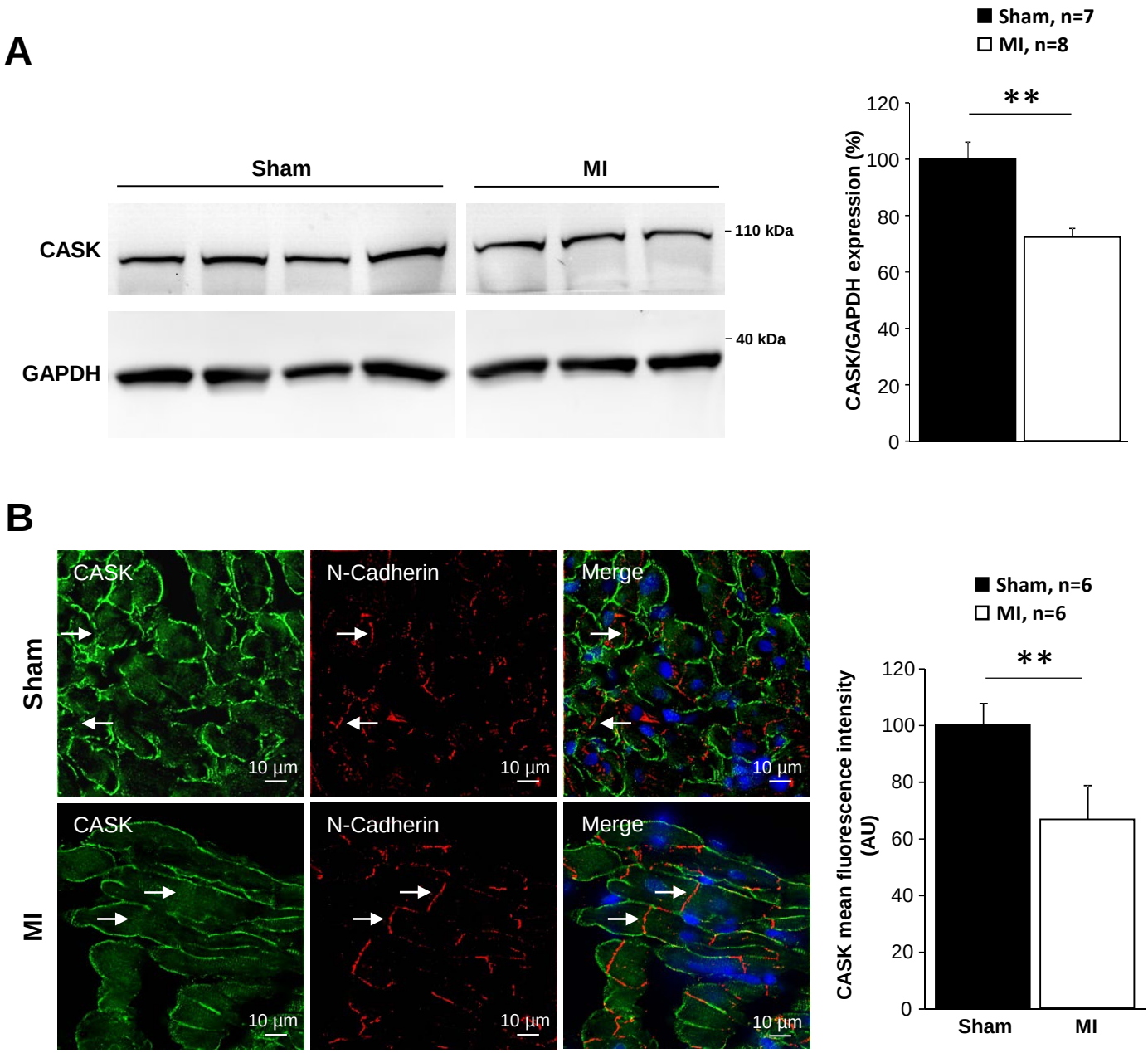

Online Figure VIII. CASK expression is reduced but its localization is unchanged in a model of chronic hemodynamic overload and dilated atria. (A) Representative western blot and histogram of the expression level of CASK normalized to GAPDH in sham and MI rats (N=3). (B) High resolution 3-D deconvolution microscopy images showing the distribution of CASK and N-cadherin in sham and MI rats and corresponding histogram of CASK fluorescence intensity from the same rats (N=3) from serial tissue slices. Arrows indicate the localization of intercalated discs. ** P<0.01.